U.S. DEPARTMENT OF COMMERCE
National Technical Information Service

PB-256 649

Precipitation Scavenging of Fossil-Fuel Effluents

Battelle Pacific Northwest Labs.

Prepared For
Environmental Protection Agency

June 1976

243008

PB 256 649

EPA-600/4-76-031
June 1976

Environmental Monitoring Series

REPRODUCED BY
NATIONAL TECHNICAL
INFORMATION SERVICE
U. S. DEPARTMENT OF COMMERCE
SPRINGFIELD, VA. 22161

RESEARCH REPORTING SERIES

Research reports of the Office of Research and Development, U.S. Environmental Protection Agency, have been grouped into five series. These five broad categories were established to facilitate further development and application of environmental technology. Elimination of traditional grouping was consciously planned to foster technology transfer and a maximum interface in related fields. The five series are:

1. Environmental Health Effects Research
2. Environmental Protection Technology
3. Ecological Research
4. Environmental Monitoring
5. Socioeconomic Environmental Studies

This report has been assigned to the ENVIRONMENTAL MONITORING series. This series describes research conducted to develop new or improved methods and instrumentation for the identification and quantification of environmental pollutants at the lowest conceivably significant concentrations. It also includes studies to determine the ambient concentrations of pollutants in the environment and/or the variance of pollutants as a function of time or meteorological factors.

This document is available to the public through the National Technical Information Service, Springfield, Virginia 22161.

TECHNICAL REPORT DATA
(Please read Instructions on the reverse before completing)

1. REPORT NO.	2.	3. RECIPIENT'S ACCESSION NO.
EPA-600/4-76-031		

4. TITLE AND SUBTITLE	5. REPORT DATE
PRECIPITATION SCAVENGING OF FOSSIL-FUEL EFFLUENTS	June 1976
	6. PERFORMING ORGANIZATION CODE
7. AUTHOR(S)	8. PERFORMING ORGANIZATION REPORT NO.
M. Terry Dana, Dennis R. Drewes, Donald W. Glover, and Jeremy M. Hales	
9. PERFORMING ORGANIZATION NAME AND ADDRESS	10. PROGRAM ELEMENT NO.
Battelle-Pacific Northwest Laboratories Battelle Boulevard Richland, Washington 99352	1AA009
	11. CONTRACT/GRANT NO.
	68-02-1729
12. SPONSORING AGENCY NAME AND ADDRESS	13. TYPE OF REPORT AND PERIOD COVERED
Environmental Sciences Research Laboratory Office of Research & Development Environmental Protection Agency Research Triangle Park, N.C. 27711	Final 6/24/74-11/28/75
	14. SPONSORING AGENCY CODE
	EPA-ORD

15. SUPPLEMENTARY NOTES

16. ABSTRACT

A numerical model for predicting the precipitation scavenging of reactive pollutants from power plant plumes has been developed. The model, called SMICK (Scavenging Model Incorporating Chemical Kinetics), calculates collection, liquid-phase chemical reaction, and desorption, if any, of multiple plume-bound pollutants as they interact with falling raindrops and are ultimately deposited on the surface. Calculations for any specific aqueous-phase kinetics mechanism can be performed with the model by expressing the mechanism in appropriate sub-routine form. The model has been tested against field experiment data.

17. KEY WORDS AND DOCUMENT ANALYSIS

a. DESCRIPTORS	b. IDENTIFIERS/OPEN ENDED TERMS	c. COSATI Field/Group
*Scavenging		13H
*Raindrops		04B
*Mathematical Models		12A
Reaction Kinetics		07D
Electric Power Plants		10B

18. DISTRIBUTION STATEMENT	19. SECURITY CLASS (This Report)	21. NO. OF PAGES
RELEASE TO PUBLIC	UNCLASSIFIED	106
	20. SECURITY CLASS (This page)	22. PRICE
	UNCLASSIFIED	5.50/2.25

EPA Form 2220-1 (9-73)

EPA-600/4-76-031
June 1976

PRECIPITATION SCAVENGING OF FOSSIL-FUEL EFFLUENTS

By

M. Terry Dana, Dennis R. Drewes,
Donald W. Glover, and Jeremy M. Hales
Battelle, Pacific Northwest Laboratories
Richland, Washington 99352

Contract No. 68-02-1729

Project Officer

Herbert J. Viebrock
Meteorology and Assessment Division
Environmental Sciences Research Laboratory
Research Triangle Park, NC 27711

U.S. ENVIRONMENTAL PROTECTION AGENCY
OFFICE OF RESEARCH AND DEVELOPMENT
ENVIRONMENTAL SCIENCES RESEARCH LABORATORY
RESEARCH TRIANGLE PARK, NC 27711

DISCLAIMER

This report has been reviewed by the Environmental Sciences Research Laboratory, U.S. Environmental Protection Agency, and approved for publication. Approval does not signify that the contents necessarily reflect the views and policies of the U.S. Environmental Protection Agency, nor does mention of trade names or commercial products constitute endorsement or recommendation for use.

ABSTRACT

The research program resulted in the development of a numerical model for predicting precipitation scavenging of reactive pollutants from power-plant plumes. Named SMICK (Scavenging Model Incorporating Chemical Kinetics), this model calculates collection, liquid-phase chemical reaction, and (possible) desorption of multiple plume-bound pollutants as they interact with falling raindrops and are ultimately deposited at the ground. Calculations for any specific aqueous-phase kinetics mechanism can be performed with SMICK by expressing the mechanism in appropriate subroutine form.

The program involved field experiments at the Centralia Steam-Electric Plant in southwestern Washington State. These show that: 1) sulfate concentrations in rainwater due to the plume's presence do not appear to be significant at downwind distances less than about 10 km; 2) ammonium, nitrate, and soluble (ortho) phosphate ion concentrations were at or near normal background levels; and 3) the only species measured which showed plume-related depostion patterns at all distances where samples were collected (0.4-11 km) were SO_2 and hydrogen ion.

Initial applications of the SMICK model included a previously-suggested aqueous-phase oxidation mechanism for SO_2, which depends strongly on the presence of dissolved ammonia. Comparisons of these predicted results with the field measurements indicate that, for aqueous-phase ammonium concentrations in the measured range, this mechanism is not adequate to account for observed rates of sulfate formation.

CONTENTS

		Page
ABSTRACT		iii
LIST OF FIGURES		vi
LIST OF TABLES		vii
ACKNOWLEDGEMENTS		ix
SECTIONS		
I.	CONCLUSIONS	1
II.	RECOMMENDATIONS	2
III.	INTRODUCTION	3
IV.	MODELING OF SCAVENGING PHENOMENA	7
V.	EXPERIMENTAL DESIGN	15
VI.	EXPERIMENTAL RESULTS	27
VII.	COMPARISON OF SMICK CALCULATIONS WITH OBSERVED DATA	57
VIII.	REFERENCES	65
IX.	NOMENCLATURE	68
X.	APPENDICES	70

Preceding page blank

FIGURES

Page

1. Schematic of Physical Interactions Modeled by SMICK. 13
2. The Centralia Steam-Electric Plant 17
3. The Centralia Precipitation Sampling Array 18
4. Precipitation Sampling Field Equipment 21
5. Rainfall Amount vs Time Measured at the Mobile Laboratory: Run F1. 30
6. Rainfall Amount vs Time Measured at the Mobile Laboratory: Run F4. 30
7. Rainfall Amount vs Time Measured at the Mobile Laboratory: Run F3. 31
8. Ground-level Rainwater Concentrations Map for SO_2, Run F1. 36
9. Ground-level Rainwater Concentrations Map for SO_2, Run F3 Boxes Show Air Concentrations in ppb 37
10. Ground-level Rainwater Concentrations Map for SO_2, Run F4 Boxes Show Air Concentrations in ppb 38
11. Measured Scavenging Rates for SO_2 (cf. (5)) as a Function of Downwind Distance. 41
12. Ground-level Rainwater Concentrations Map for Sulfate, Run F3. . . 44
13. Ground-level Rainwater Concentrations Map for Sulfate, Run F4. . . 45
14. Ground-level Rainwater Concentrations Map for H^+, Run F3 46
15. Ground-level Rainwater Concentrations Map for H^+, Run F4 47
16. Cross-Plume Rainwater Concentrations Profiles in Tenino Area ($x \sim 10$ km). 49
17. Scanning Electron Photomicrograph of a Particle From Mobile Rain Sample 71B. The Diameter of the Particle is about 4.9 μm. 55
18. Scanning Electron Photomicrograph of Particles from Mobile Rain Sample 82C. The Diameter of the Spherical Particle in Right Center is about 5.5 μm 55

TABLES

Page

1. Sampling Areas. 20
2. Chemical Analysis Methods for Pollutants Measured and Nominal Low Detection Limits. 26
3. Plant Operation and Emission Data 28
4. Fixed Site Collection Times 29
5. Rainfall Rates Summary. 29
6. Raindrop Size Frequency Distributions 33
7. Wind and Temperature Data 33
8. Scavenging Rates for SO_2: Comparison of Present Results with Those of the Previous Studies 40
9. Meteorological and Source Conditions Relevant to Scavenging Rate Comparisons 42
10. Measured Air Concentrations of NH_3 and O_3 51
11. Measured Air Concentrations of SO_2. 52
12. Results of Electron Microscope Analyses of Filtered Rain Samples. . 54
13. SMICK Calculations with Scott and Hobbs Mechanism: Uniform Gas Phase SO_2 Concentration 59
14. Calculated Plume Centerline Rainwater Concentrations: SMICK (Scott and Hobbs; K=0.0017 sec^{-1}) and EPAEC (SO_2 only) 60
15. Sample SMICK Plume Centerline Rain Concentration Calculations with Scott and Hobbs Mechanism: Run F3 Input Data P_{CO_2}=311 ppm. 62
16. Cross-Plume SMICK Rain Concentration Calculations: Run F3, Tenino (x∿10 km) Area, K=0.0017 sec^{-1}; P_{NH_3}=1 ppb; P_{CO_2}=311 ppm. 64
17. Rain Sample Concentration Data: Run F1, December 6, 1974 71
18. Rain Sample Concentration Data: Run F3, December 10, 1974. 72
19. Rain Sample Concentration Data: Run F4, December 12, 1974. 73
20. Rain Sample Concentration Data: Run F5, December 15, 1974. 74
21. Concentration Results-Mobile Samples (and Associated Fixed Sites): Run F3, December 10, 1974 75
22. Concentration Results-Mobile Samples (and Associated Fixed Sites): Run F4, December 12, 1974 76
23. Concentration Results-Mobile Samples: Convective Shower, December 12, 1974 77

Page

24. Values of the Equilibrium Constants (Equations 6b-14b) used in SMICK calculations with the Scott and Hobbs Mechanism (T=298K). . . .81

25. Input Data for Sample Calculations. 94

26. Sample Calculations Showing ΔZ Variation. 94

ACKNOWLEDGEMENTS

We are grateful for the cooperation and assistance of personnel of Pacific Power and Light Company, operators of the Centralia Steam-Electric Plant. In particular, Bob Davis and Gordon Strom of that company provided coordination which made our field operations on the plant property a success.

We appreciate the kind help of Professor Donald Adams of Washington State University, who provided the wind and temperature data from the meteorology tower.

Battelle-Northwest personnel who contributed significantly to the overall project include Sam Henderson, R. E. Kerns, and J. W. Sloot.

SECTION 1

CONCLUSIONS

A predictive model for the scavenging of fossil-fuel effluents was developed. The initial application of this computer model has been to the sulfur compounds -- SO_2 and oxidized ionic species, particularly sulfate. The development of the scavenging model incorporating chemical kinetics (SMICK) came about by extension of the existing SO_2-only model (EPAEC) to include other species, and chemical reactions among them occurring within raindrops during their trajectories through a plume. Comparisons of the calculated results with experimental data, when a liquid phase oxidation mechanism involving ammonia is employed, indicate that this mechanism is insufficient to explain observed sulfate formation rates in the plume-and-raindrops situations tested.

The data from the field experiments at the Centralia Steam-Electric Plant, the first taken there during normal operation of the coal-fired facility, show that: 1) sulfate concentrations in rainwater due to the plume's presence do not appear to be significant at downwind distances less than about 10 km; 2) ammonium, nitrite, nitrate, and soluble (ortho) phosphate ion concentrations were at or near normal background levels; and 3) the only species measured which showed plume-related deposition patterns at all distances where samples were collected (0.4-11 km) were SO_2 and hydrogen ion.

The field program employed, in addition to fixed site collectors, short-time sampling with mobile collectors. Some of the large-volume rain samples were filtered and subsequently examined for insoluble particle content by scanning electron microscopy (SEM). The mobile sampling can be useful for studying short-time rainwater concentration fluctuations, and the SEM analysis shows great promise as a means by which fossil-fuel effluent particles may be identified and counted, and their scavenging properties determined.

SECTION II

RECOMMENDATIONS

The modeling of scavenging of reactive fossil-fuel plumes should be continued. The basic framework of SMICK is amenable to the testing of many liquid-phase reaction mechanisms, and -- with the addition of an existing reactive plume model -- the role of gas-phase reactions can be examined as well. The major effort of the current contract was concerned with development of the computational algorithm; various scavenging and reaction mechanisms can be tested without major modifications.

The findings of this phase of the research program demonstrate that there is a strong need for experimental measurements of ammonia solubility in water at low concentrations. Because of the evidence of marked deviations between observations and calculated ammonia solubility, and because of the intrinsic importance to several proposed mechanisms of SO_2 oxidation, these measurements should be performed prior to any further speculation regarding the role of ammonia in SO_2 oxidation processes.

There is a need to examine the composition and scavenging efficiencies of small insoluble effluent particles which escape the electrostatic precipitators of fossil-fueled facilities. This can be accomplished through scanning electron microscope analysis of filtered rain samples; in principle, the rainwater content and particle size distributions can be determined at various downwind travel times. These results can be compared with measured or inferred source strengths and particle size spectra to arrive at an assessment of the scavenging rates.

Large-area mobile precipitation samples can be used in future research to provide a reasonably good measure of the deposition patterns of many soluble effluents. These also can be used to examine short-term concentration fluctuations, and can provide the large water volumes needed for sensitive insoluble particle analysis.

SECTION III

INTRODUCTION

The atmospheric effluents which result from the use of fossil fuels generally consist of the gaseous products of ordinary combustion of organic matter -- CO, CO_2, NO, NO_2, H_2O, SO_2 -- and the more complicated and less prevalent combustion products consisting of small amounts of various contaminants. These contaminants -- defined as not being a necessary aspect of the fuel -- are generally inorganic compounds and elements found in varying amounts in the earth's crust, such as oxides of silicon, iron, aluminum, and trace quantities of heavy metals. The relative abundances of the various pollutant species in the atmospheric effluent stream depend on the type of fuel used and the means and efficiency of combustion and control measures.

The atmosphere and biosphere have been capable of coping with large natural occurrences of the release of typical fossil-fuel effluents. For example, the natural emission of sulfur dioxide from volcanoes in normal times has been estimates at about 10^{12} grams annually.[1] The increasing use of fossil fuels by humanity throughout the ages has, however, brought us to the point where the anthropogenic contribution of SO_2 to the atmosphere is of the same magnitude.[2] The difficult question of when (if not already) these and like emissions begin to affect health and quality of life must be faced, in order that the overall impact of human activities may be recognized in a timely way, and that alternatives to present developments may be effectively considered.

The toxicities of the effluent gases (with the exception of H_2O) have been well demonstrated; the task of removing them is a difficult one, however, and the environmental question is basically one of assessing the damage which comes about through their release, and then attaching limits to the releases. Of course, the assessments direct the development of control

mechanisms where necessary. The particulate effluents are most easily controlled; in fact, a large fraction of the mass of fly ash particles resulting from most types of fossil-fuel combustion can now be removed by electrostatic precipitation. Nevertheless, the effluent streams contain large *numbers* of very small particles, whose effect on the environment may be felt in a manner more indirect than that of the gaseous oxides.

The interactions between pollution and the atmosphere have been researched extensively, particularly in the areas of transport and diffusion, dry deposition, and precipitation scavenging. Each of these classes of interactions has generally been treated independently of the others. Of late, however, the overall *fate* of pollutants has been of concern; that is, answers are being sought to the question of whether pollutants change chemically and/or physically in time, and under what conditions. The changes can profoundly affect the rates of removal from the atmosphere. Probably because experimental measurements are easiest in fair weather, the fate of certain pollutants is better understood for non-precipitating conditions. For example, SO_2 conversion rate estimates and information about the coagulation of particles have been derived from aircraft measurements under fair weather conditions only.

The chemical conversions which may occur among fossil-fuel pollutant plume constituents under precipitation conditions are probably more complicated; in addition, experimental measurements are generally confined to the ground level. There is evidence that the molar concentrations of sulfate in rainfall at ground level are comparable to those of SO_2, even at relatively short distances down wind of a coal-fired source.[3] The implied rates of SO_2 conversion -- if it is a gas-phase process -- are much faster than those proposed for fair-weather conditions. The possibilities are then open for, among others, 1) an accelerated gas-phase reaction process, 2) a liquid phase reaction process in precipitation, 3) a liquid phase process in cloud droplets and subsequent efficient scavenging of cloud drops by precipitation, or 4) combinations of the above.

It is the objective of the present research to model precipitation scavenging of fossil-fuel effluents, accounting for chemical conversions as well as the better known physical processes. The primary interest is with the SO_2 - sulfate reaction process, for the following reasons.

1) The fate of SO_2 is of particular concern because it is the currently recognized major atmospheric effluent of fossil-fuel combustion in terms of environmental impact.

2) Our experience with the modeling of scavenging of gases -- and particularly SO_2 -- makes it natural to begin a modeling program including chemical reactions with the pollutant whose scavenging properties are otherwise best understood. In addition, the framework of the developed gas scavenging model is amenable to generalization to several species with reactions occurring among them.

3) A number of atmospheric conversion processes have been proposed which concern themselves with the SO_2-sulfate problem. It is important that means be developed whereby these processes can be tested under conditions which exist in real fossil-fuel plume and precipitation situations.

Furthermore, the atmospheric and plume conditions which promote chemical conversions in precipitation conditions are not well known. That is, all currently proposed mechanisms which involve catalysts by some plume or natural constituent may prove inadequate to explain observed precipitation concentrations of the materials of interest. Therefore, it is considered an important objective of the study to conduct field measurements concerned with a number of pollutants, some of which may be important as catalysts, and some of which may be of significant environmental concern in their own right.

This report documents the year's work, which consists of the development of a model for the scavenging of chemically reacting plume-borne effluents and the conduct of a field measurement study of precipitation

deposition of a number of pollutants from a large coal-fired power plant. The report is generally in three parts, describing: the development of the model (Section IV), the methods employed in and preliminary results of the field study (Sections V and VI), and some initial applications of the model to real experimental situations from the current field study and past ones (Section VII).

SECTION IV

MODELING OF SCAVENGING PHENOMENA

During the contract period the mathematical modeling of scavenging phenomena has progressed in two basic areas: improvements in the gas-scavenging code, EPAEC, developed under a previous contract,[3-4] and the formulation of a revised code, SMICK, to calculate scavenging of multiple, reacting plume constituents. Progress in each of these areas is summarized individually in the following paragraphs.

REVISIONS OF EPAEC

The computer code EPAEC (described briefly in Appendix C, and in detail elsewhere[3]) calculates scavenging of material from a Gaussian plume by raindrops falling along slanted trajectories; the drop-pollutant interaction is considered to be purely a physical (or pseudophysical) process, where no irreversible chemical reactions occur within the aqueous phase. Although a first-order chemical reaction within the gaseous phase is possible, modifications of the plume by the rain are assumed to be negligible. Plume loft is incorporated into the model in rudimentary fashion only, providing for either a linear loft rate, or a level plume established at a predetermined virtual release height.

EPAEC was found to perform well for the conditions experienced in the previous study.[3] Later applications under the present contract, however, showed the numerical algorithm to be unstable under some circumstances, which often involved high, confined plumes containing gases of relatively low solubility. Because of this difficulty, a theoretical stability analysis of the basic Runge-Kutta algorithm employed in the code was performed. Noting that the Runge-Kutta algorithm is employed in EPAEC to obtain finite-difference approximations (FDA's) to solutions of the basic drop-response equation

$$\frac{dc}{dz} = \frac{3K_y}{av_z}(y_{Ab} - H'c) \quad , \tag{1}$$

it was found that the algorithm should, indeed, tend toward instability under the following conditions:

$$\left| 1 + \Delta z \ \frac{\partial\left(\frac{dc}{dz}\right)}{\partial c} \right| < 1 \quad . \tag{2}$$

The nomenclature in the above forms is given as follows:

- a = raindrop radius, ℓ
- c = concentration of pollutant in raindrop, moles/ℓ^3
- H' = solubility parameter, ℓ^3/mole
- K_y = mass-transfer coefficient, moles/$\ell^2 t$
- v_z = terminal velocity of fall of raindrop, ℓ/t
- y_{Ab} = mole fraction of pollutant A in local gas phase
- z = distance above ground at stack base, ℓ
- Δz = spacing of computation grid, ℓ.

Inequality (2) indicates that, at set values of Δz, numerical instability should be expected for low solubilities (high values of H'), small raindrops, and high mass-transfer coefficients. Since the step size Δz is easily adjustable using the Runge-Kutta algorithm, a simple solution to this instability problem is to provide for an automatic adjustment of the step size within EPAEC to satisfy criterion (2). This measure, however, was found to be only partially satisfactory. While successfully stabilizing the algorithm, the modification often reduced Δz to such small values that execution times became prohibitively large. In view of this difficulty, alternative solutions to the instability problem, involving other finite differencing techniques, were explored. These included:

1) application of predictor-corrector methods,

2) application of successive perturbation techniques,

3) use of second-order single-step algorithm suggested by Liniger and Willoughby[5],

and 4) application of the exponential method of Sherwood and Berman[6].

Techniques 2-4 were rejected, for the present, because they either necessitated numerical differentiation of the forcing function y_{Ab}, or were judged too clumsy for anticipated multicomponent applications in the SMICK code, which was expected to employ a similar algorithm. Predictor-corrector methods possess neither of these difficulties; on the other hand, they do tend to become unstable under specific conditions. These conditions are not so severe as those posed by the Runge-Kutta method; in fact, many predictor-corrector methods possess the additional advantage of being substantially more efficient than their Runge-Kutta counterparts. Moreover, predictor-corrector methods provide a more direct estimate of numerical deviations from the true solutions, allowing a relative economization of any step-size modification imposed for stability maintenance.

Because of the above features, a predictor-corrector algorithm was formulated for use in a revised version of EPAEC. The technique chosen was a modified version of Hamming's[7] method, which possesses a number of desirable features, including a fourth-order truncation error and relative absence of parasitic solution effects. Experience with this revised code to date has indicated that the previous problems have been countered successfully under most conditions, although a moderate reduction in Δz is still necessary to maintain stability under some circumstances. In addition to including a provision for reducing Δz, the new algorithm also increases Δz where conditions permit; this often results in a shorter computation time than is required by the old method. Examples of Δz modifications during integration are shown in Appendix D.

In addition to incorporating the more sophisticated predictor-corrector algorithm, EPAEC was also revised to account for plume loft in a more satisfactory fashion. The revised formulae of Briggs[8], used in the earlier version of the code, are employed in a more exact manner to allow a "bent-over" plume, rather than the more simplistic concepts employed by the

earlier model. Conceptually, this was not a difficult modification. Because of its effect on the relationships between the plume position and raindrop trajectories, and the associated structure of the finite difference grid locations, however, this modification has resulted in a substantial restructuring of the computer program listing.

MULTICOMPONENT SCAVENGING FROM PLUMES: THE FORMULATION OF SMICK

As indicated previously, EPAEC focuses upon the scavenging of a single plume constituent only. For an advanced analysis of pollutant scavenging in power plant plumes it is desirable to possess an extended diagnostic model which provides for the wet removal of multiple reactive components; the computer code SMICK (Scavenging Model Incorporating Chemical Kinetics) has been formulated to fulfill this requirement.

The basic properties of SMICK can be presented best by considering the basic steady-state equations of continuity for the two phase (rain-air) system of interest[9]:

$$- \nabla \cdot \rho_{Ax} \bar{v}_{Ax} + w_A + r_{Ax} = 0 \quad \text{(aqueous phase)} \tag{3}$$

and

$$- \nabla \cdot \rho_{Av} \bar{v}_{Ay} - w_A + r_{Ay} = 0 \quad \text{(gaseous phase)}, \tag{4}$$

where

A = component index = $1,2,\ldots,N$

$\bar{v}_{Ax}$, $\bar{v}_{Ay}$ = velocity vectors for component A in rain and air, ℓ/t

r_{Ax}, r_{Ay} = reaction rates for component A in rain and air, moles/$\ell^3 t$

w_A = interphase transport rate of component A, moles/$\ell^3 t$

ρ_A = molar concentration of component A in space moles/ℓ^3

Both SMICK and EPAEC assume that w_A is negligibly small in (4), and both require an externally-supplied solution of this equation* in order to solve (3) for aqueous-phase concentrations. In contrast to EPAEC, which assumes $r_{Ax} = 0$ and considers only a single component (N=1), SMICK allows for multiple components ($N \geq 1$)** and provides for arbitrary expressions to describe aqueous-phase reaction behavior.

The simultaneous mass-transfer and chemical-reaction process characterizing a particular microphysical model of interest in incorporated into the overall code as follows: first the mechanism is separated into its individual steps, and is expressed in terms of simultaneous equations, which may be algebraic expressions, first-order ordinary differential equations, or both. (Note that (1), employed in EPAEC, is such an equation but the relative simplicity of this code requires only one such expression.) Upon formulating the defining equations, they are coded in a FORTRAN subroutine which provides the appropriate microphysical parameters when interrogated by the calling program, SMICK. With this arrangement, virtually any liquid-phase reaction mechanism can be employed with the code in a relatively simple and straight-forward manner.

The multiple interactions defined in the above fashion are treated by solving simultaneously the corresponding multiple differential equations using the predictor-corrector algorithm in a manner similar to that employed for the single equation in EPAEC. All of the improvements described earlier for EPAEC have also been adapted into SMICK, and one should note that SMICK can be executed to produce the same results as EPAEC, if it is constrained to the special case, N=1.

---

* This externally-supplied solution is presently the Pasquill-Gifford bivariate-normal plume equation in both SMICK and EPAEC. This can be modified easily, however, by simple exchange of the subroutines providing the solutions.

**The present code limits N to 10 components. This number can be extended easily by suitable replacement of DIMENSION statements, however.

The physical interactions modeled by SMICK are presented schematically in Figure 1. As indicated by this diagram, the code allows for the capture of both gases and aerosols by the raindrops, in which the material may react, desorb, or deposit on the ground.

It should be emphasized that the high versatility in describing liquid-phase reaction phenomena in SMICK is not at the present time matched by a similar capability for components in the gas phase. Since the plume model incorporated by this code is expressed in subroutine form, it may be exchanged easily with one incorporating more sophisticated gas-phase reaction kinetics. Such a measure, however, would result in intolerable increases in execution time, and is judged to be unwarranted for this project. A more viable alternative is to obtain computer solutions to an appropriate reactive plume model, and store these solutions in a three-dimensional matrix, corresponding to the spacially-varying concentration field. The SMICK code can then be executed in its usual manner, after modifying the plume subroutine to a three-dimensional interpolation, which calculates plume concentrations at any point from the base data in the matrix. A three-dimensional interpolation algorithm has been formulated to accomplish the above function, and two reactive plume codes - formulated under other programs - are ready for use in this capacity. The first of these is PROTEUS, a moderately rigorous and versatile K-theory model; the second is STRAC, a code based upon the simplified concept of a quasi-Gaussian plume, which possesses the advantage of comparatively rapid execution times. At the present time neither STRAC nor PROTEUS have been operated with SMICK in this capacity.

Application of SMICK for Scavenging Analysis

The intention of this program is to apply SMICK as an aid in validating or rejecting postulated mechanisms of microphysical scavenging behavior. In accomplishing this, the particular mechanism of interest is expressed in subroutine form and incorporated with the code as described earlier. The code is then executed for conditions corresponding to field experiments performed under this program, and pollutant concentrations in rain predicted

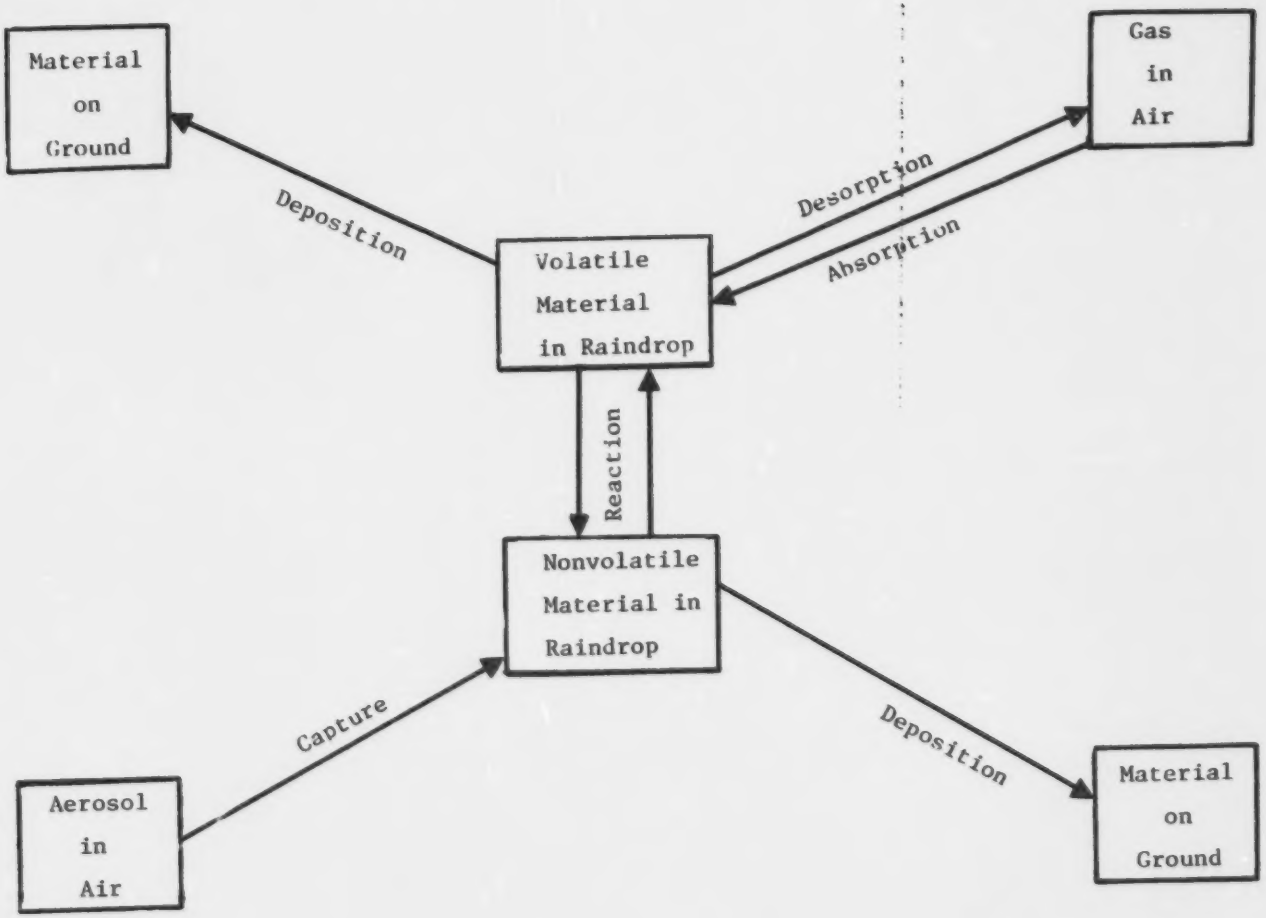

FIGURE 1. SCHEMATIC OF PHYSICAL INTERACTIONS MODELED BY SMICK.

by the code are compared with those actually measured. In such an application it should be recognized that, while disagreement between observed and predicted values provides a strong basis for rejection of a given mechanism, the converse is untrue. This is simply because the complex conditions leading to wet deposition of some materials allow the possibility that the same final circumstances might be predicted by a variety of diverse microphysical mechanisms. While this feature does not detract totally from the above approach to mechanistic examination, one must be cognizant of its existence in applying this method for analysis of the scavenging process.

Several mechanisms for SO_2 conversion and scavenging exist in the literature; it is the intent of this program to proceed systematically through these mechanisms in the above manner in an attempt to ellucidate their applicability. At the present only one mechanism, that of Scott and Hobbs[10], has been examined in this fashion. A description of the application of SMICK and this oxidation mechanism to experimental situations is included in Section VII.

SECTION V.

EXPERIMENTAL DESIGN

A field study was conducted to provide a data base of pollutant measurements for use in the modeling analysis. For present purposes these are primarily the sulfur compounds but it was desirous to examine the precipitation (and some gas-phase) concentrations of a number of inorganic pollutants, some of which are potentially important in the sulfur oxidation process. In addition, the pollutants NO_2^-, NO_3^-, and PO_4^{3-} are candidates for possible future scavenging modeling. Initial experimental examinations of insoluble pollutants were conducted as well; this effort took the form of electron microscope analyses of particles collected by filtration of rain samples.

The field work was undertaken in December, 1974, in the vicinity of the Centralia Steam-Electric Plant in southwestern Washington State. Our experience at that site includes two previous experimental series. Those provided a considerable amount of SO_2 and sulfate concentration data useful in conversion studies, but both were inadequate in certain respects. A study under a previous EPA contract[3] in the spring of 1972 was concerned primarily with SO_2 scavenging and an initial assessment of the relative concentrations of SO_2 and sulfate in rainwater. Concentrations of the nitrogen compounds and phosphate were not measured at that time, and the pH data were not extensive enough to characterize the H^+-SO_4^{--} relationship in individual samples. Some further work based on this study, including a rather qualitative examination of SO_2-sulfate conversion mechanisms, has been published[11]. A brief field effort in early 1974, involving only one experiment, concentrated on sampler-surface SO_2 desorption (touched on briefly in the earlier study) and testing of new sampling methods. Nitrogen compounds and pH were examined in more detail, but the sampling array was limited to near the power plant[12]. Both of the earlier Centralia studies were affected by nontypical operating characteristics of the power plant itself; only one of the two units was operating in each case, and electrostatic precipitator problems limited output. The 1974 session was also affected by the addition of sulfur trioxide to the stack

effluent stream; this was done to increase the precipitator efficiency during the construction of new precipitators. In view of all these limitations and special circumstances, the December 1974 field trip was mounted in an effort to obtain more complete measurements under normal plant operating conditions.

The Centralia Steam-Electric Plant (Figure 2) is a dual-unit, coal-fired facility with a maximum output of about 1300 Mw. The coal (mined locally) is a subbituminous type with a sulfur content averaging 0.55%. The topography surrounding the plant is rugged, with heavily forested hills rising to within 50 m of the stack tops within a few kilometers in the normal downwind direction. Precipitation sampling sites are easily located, however, on clearcut areas within 7 km, and on natural prairie areas beyond. The general wind direction during rainy weather (from the south) is such that extensive background levels of the pollutants of interest are rare; the plant and its environs are an excellent location for examination of fossil-fuel effluent effects.

PRECIPITATION SAMPLING

The primary objective of the field study was to collect precipitation samples in the area under the plume at distances from 0.4 to 11 km downwind. The fixed collection sites numbered about 90, and were arranged as shown in Figure 3. With the exception of an area of heavy forest between sites 72 and 73, and a coal mining region generally east of 61 and south of 74, the array covered the accessible area normally affected by the power plant plume. The sampling at the fixed sites was facilitated by the use of a single precipitation collector, one which is designed to freeze the collected rainwater and thus preserve the sample to allow any number of separate chemical analyses to be performed[13]. The sampler consists of a plastic funnel of area 325 cm^2 connected to a plastic bottle capable of holding and preserving 1.5 cm of rainfall up to 12 hours. In contrast to the 1972 study, where separate collectors were used for SO_2, sulfate, and H^+, the current samplers were much easier to handle, thus allowing a far greater number to be deployed by fewer personnel.

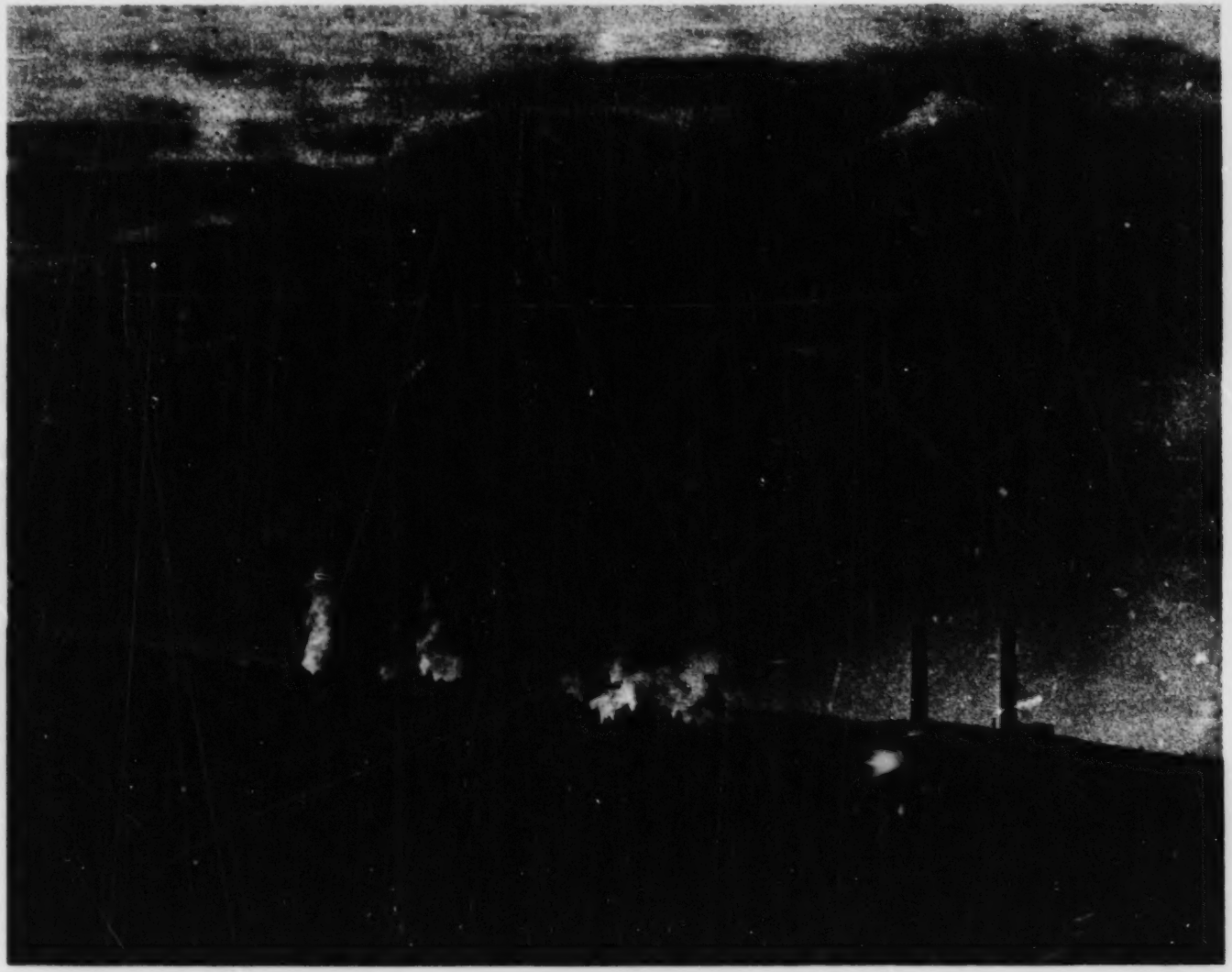

FIGURE 2. THE CENTRALIA STEAM-ELECTRIC PLANT.

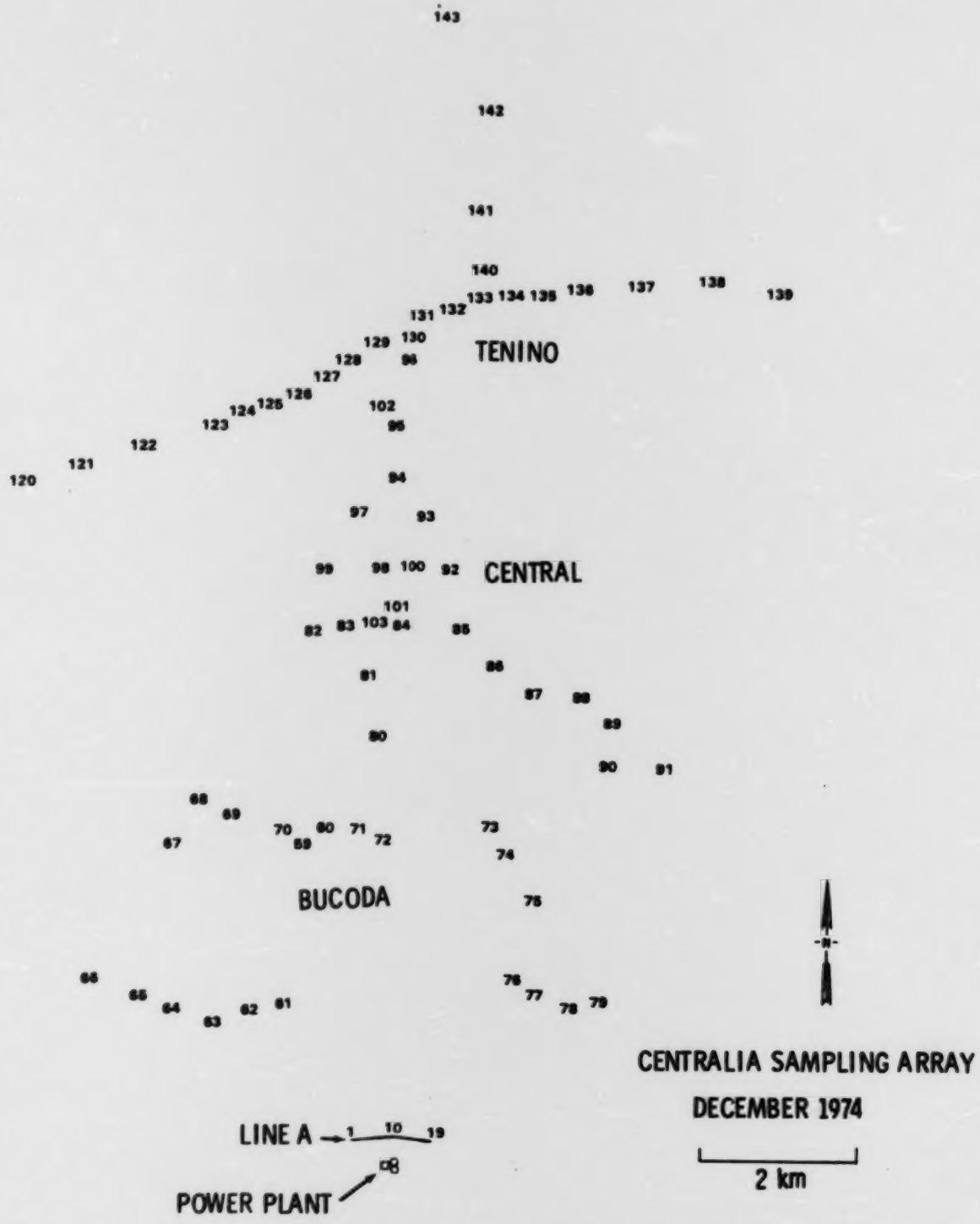

FIGURE 3. THE CENTRALIA PRECIPITATION SAMPLING ARRAY.

The fixed site array was divided into five areas listed in Table 1. These coincide generally with the assignment of service personnel and approximate lines of samplers at various distances downwind. (The Line A area is so named because it coincides almost exactly with Line A of the 1972 field study. The site numbers, however, are different.) For convenience, these areas will be referred to by name in the balance of this report.

Mobile Sampling

Two mobile precipitation collectors were outfitted to provide short-time (as short as one minute) samples at locations which could be selected as the experiment went on. One of these is shown in Figure 4; it consists of a large plastic-lined funnel of area 1 m^2 mounted on cartop with plumbing to the inside where samples could be bottled and frozen immediately. One of the samplers had a provision for pH measurements (Figure 4); real-time pH measurements allowed for location of the mobile site in relation to the power plant plume, as observed by the presence of acid rain. In general, the pH-capability sampler would locate the plume centerline, and its operator could direct the other mobile sampler operator by radio to a suit-

Table 1. SAMPLING AREAS

Area Name	Mean Distance from Plant, km	Site Numbers
BKG	3.4[a]	BKG
Line A	0.4	1-19
Bucoda	4.5	59, 60, 67-79
Central	8.0	80-103
Tenino	11.0	120-145

[a]Upwind (south)

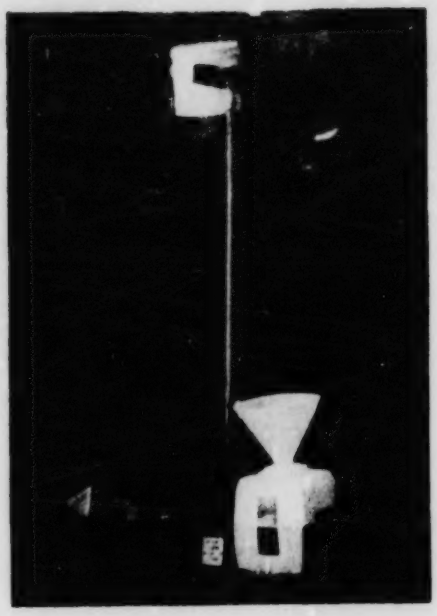

a

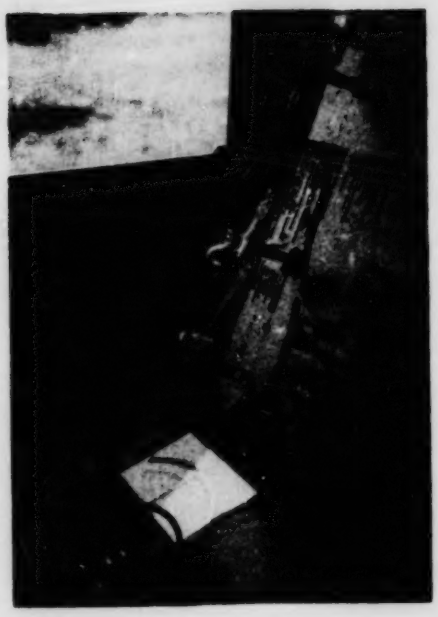

b

FIGURE 4. PRECIPITATION SAMPLING FIELD EQUIPMENT. a) FIXED-SITE SAMPLING STATION WITH ICE CREAM CARTON (TOP), SO_2 BUBBLER (LEFT), AND STANDARD FREEZING COLLECTOR. b) MOBILE pH MEASUREMENT EQUIPMENT.

c

d

FIGURE 4 (CONTINUED). c) MOBILE PRECIPITATION COLLECTOR (AT SITE 71), WITH FIXED-SITE GEAR IN FOREGROUND. d) BATTELLE MOBILE LABORATORY AT THE CONTROL CENTER, SITE 9.

The mobile sampling capability was included in the experiment design for several reasons:

1) Measured concentration in short-time samples could be compared with accompanying fixed site concentrations to help identify any sampler-related problems involving funnel-surface desorption of SO_2, speed of freezing, or dry deposition.

2) A series of short-time samples, taken sequentially, could give indication of fluctuations in precipitation concentrations due to plume movements, rain rate variations, or variable chemical reactions.

3) The mobile samplers could simulate a line of fixed sites across the plume through a rapid traverse of the plume (the time between successive samples at different locations could be as short as five minutes); an attempt at this was intended as a test of the potentials for mobile samplers to replace fixed sites in future field work.

4) The samples thus derived would in principle be less susceptible to contamination by local sources of pollution; these could be filtered for insoluble particle analysis.

Other Precipitation Sampling

A third type of bulk precipitation sampler was used at selected sites. This was merely a plastic bag contained in a paper ice cream carton (Figure 4). Intended for metals analysis by atomic absorption spectrophotometry, the samples thus collected could be separate from the other fixed site samplers. The latter required less care in handling because the inorganic pollutant concentrations are presumably in the part per million range, rather than the expected part per billion range for the metals.

An attempt was also made to examine the insoluble particle content of individual raindrops. This was done by exposing fine pored (0.1 micron) membrane filters directly to falling rainfall, in locations which were expected to be near the plume centerline. These filters were saved for examination by electron microscopy.

AIR SAMPLING

A limited number of air concentration measurements were made by use of battery driven bubbler-impinger samplers. These were designed primarily to provide background measurements of SO_2, O_3, and NH_3. The latter two have been proposed as catalysts in the SO_2-sulfate conversion process. Several bubblers were also positioned downwind of the plant to provide spot checks of ground-level SO_2 concentrations in the plume. The absorbing reagents (impinger solutions) were as follows: for SO_2, tetracholormercurate (TCM); for O_3, an alkaline potassium iodide solution; and for NH_3, a slightly acid solution. Analysis methods are discussed below.

SUPPORTING MEASUREMENTS

The Battelle mobile laboratory (Figure 4) was utilized to provide a field base of operations at the center of Line A about 400 m north of the north stack. At that site (site 9) were located two tipping bucket raingauges, one with standard 0.25 mm (0.01 inch) increments, and one fitted with a larger funnel to provide 0.04 mm increments. The raingauges provided an overall measure of the rain amount and rate to characterize the runs, and also provided a time record of rain for comparison of site 9 amounts with the amounts collected in the fixed samplers at other locations. The faster response gauge was useful in comparing rainfall rates with those calculated from raindrop size spectra. The latter were derived from raindrop spot size measurements from exposed sheets of water sensitive, calibrated paper.

No attempt was made to measure wind characteristics; we chose to rely on wind data collected at stack top height on the plant-operated meteorology tower, which was located approximately 1.3 km northwest of the power plant. These data proved to be adequate for modeling input for the 1972 study[3]: the added expense of installing our own instrumented tower was thus not deemed practical for the present study. The reliance on the plant data caused some problems, however, as is noted in Section VI.

EXPERIMENTAL PROCEDURE

A supply of dry ice was kept available for stocking precipitation collectors at a storage location in the town of Centralia. When a rain was forecast as imminent, or when rain was already occurring at the start of a work day, the collectors were stocked (normally taking about a half hour), and the Tenino and Bucoda area personnel dispatched. The field director, who maintained Line A and the background site, prepared those samplers and made a visual check on wind and rain conditions at the mobile laboratory site. His radio report to each sampling area operator either commenced sampler setout or called a delay until conditions were proper. The Central area operator (mobile/pH operator) either deployed samplers in his area or proceeded to make short-time collections. The second mobile sampler was employed in the Bucoda area; short-time samples from this sampler were begun (with radio guidance) after that area's fixed sites were deployed. At the conclusion of rainfall, onset of darkness, or otherwise after at least 0.15 cm of rainfall were collected, the recovery of fixed samples began. Mobile sampling continued as long as useful thereafter, depending on the fixed-site obligations of the mobile operators.

CHEMICAL ANALYSIS

All chemical analyses of rain samples and air samples of NH_3 and SO_2 were conducted at the Richland laboratories of Battelle-Northwest. Standard automated methods for analysis of SO_2, SO_4^{--}, NO_2^-, total inorganic fixed nitrogen (TIFN=$NO_3^- + NO_2^- + NH_4^+$), NH_4^+, and PO_4^{3-} are listed in Table 2,

Table 2. CHEMICAL ANALYSIS METHODS FOR POLLUTANTS MEASURED AND NOMINAL[a] LOW DETECTION LIMITS

Pollutant	Method	Lower Detection Limit (g-moles/cm^3) x 10^9
SO_2 (dissolved)	Modified West and Gaeke[15]	0.1
$SO_4^=$	Methylthymol Blue[16]	2.0
NO_2^-	Saltzmann[17]	0.03
NO_3^-	Phenoldisulphonic Acid[16]	0.3
NH_4^+	Phenoldisulphonic Acid[16]	0.35
H^+	Glass Electrode	(±0.1 pH unit)

[a]Sensitivities for individual analysis sessions vary; these are indicated in the chemical analyses results in Appendix A.

along with nominal minimum detectable concentrations. The sensitivity limits vary somewhat, depending on sample quality and variations in reagents, etc.; actual sensitivity limits for given days of operation are indicated in the tabulations of measured concentrations, Appendix A. It was anticipated that NH_4^+ would be measurable with a specific-ion electrode, but experience with the probe and improvements to the automated method revealed better sensitivity for the latter. (The improvement noted came about through the use of a longer colorimeter flow cell.) The bubbler solu-

tions were examined in the same manner as the rain samples, with the exception of the ozone bubbler samples, which were done in the field via the alkaline potassium iodide method[14]. This method produces a stable iodide which is later liberated in the form of iodine by the addition of a reagent.

SECTION VI.

EXPERIMENTAL RESULTS

Three experiments involving significant collection of precipitation were accomplished at Centralia during the December, 1974, field trip. The experiments to be discussed here are called F1, F3, and F4. As a convention, we routinely number any experiment which results in some data collection. In this connection, F2 was an aborted precipitation run -- no rain occurred, but air concentration measurements were made. A similar situation arose in the case of Run F5, where only a few marginally small rain amounts were experienced.

Relevant power plant operating data are listed in Table 3. During F1 the electrical output was essentially at capacity; the other runs were accompanied by a slightly reduced firing rate for one of the units. The hourly electrical output was very uniform during the times of precipitation sampling in all cases, and it was assumed that the coal firing was uniform as well (the coal consumption data are hourly averages computed from daily totals).

There were slight variations among the runs in the number of fixed sampling sites active. This is indicated in the concentration tabulations in Appendix A. The timing of site deployment and recovery is shown in Table 4. The times of sampling of all the sampling areas coincided well; this was facilitated by having continuous radio contact between all personnel. It should be noted -- and this is important in interpreting the concentration results -- that the times of rainfall were generally different from the total sampling times. For all practical purposes, rain fell over the entire array for the duration of sampling on run F3. The other two runs contained rain periods with dry times between. Figures 5-7 are plots of rain amount vs time as measured at the mobile laboratory, site 9. A comparison of rainfall rates measured at site 9 and at apparent plume centerline fixed sites in each area is shown in Table 5. Run F1 is not included because the showers were scattered and rainfall amounts varied considerably over the array. Very little rain fell at site 9, but significant amounts

Table 3. PLANT OPERATION AND EMISSION DATA[a]

Run	Hours PST	Hourly Averages: Electric Power[b] Mw	Coal Burned[c] metric tons	Sulfur Emitted[d] gram moles/sec
F1	0900-1700	1197 ± 1%	680	32.9
F3	1200-1700	903 ± 5%	535	25.4
F4	1000-1500	934 ± 2%	530	25.7

[a] From log sheets provided by plant management

[b] ± indicates extreme variations

[c] Hourly average based on daily total

[d] Based on a sulfur content of 0.56% derived from average of daily assays taken between 12-1-74 and 12-11-74.

Table 4. FIXED SITE COLLECTION TIMES

Run	Date	Inclusive Sampling Times - First Out to Last In				
		BKG	Line A (1-19)	Bucoda (61-79)	Central (80-102)	Tenino (120-144)
F1	12-6-74	0911-1603	0929-1503	0916-1524	0935-1542	0905-1643
F3	12-10-74	1340-1645	1300-1558	1233-1643	1245-1602	1230-1632
F4	12-12-74	1055-1516	0958-1413	1014-1447	1012-1345	1028-1431

Table 5. RAINFALL RATES SUMMARY

Run[a]	Rain Time Fraction[b]	Site 9 J, mm/hr	J (Collected rain[c])/J (Site 9 gauge)				
			BKG	Line A	Bucoda	Central	Tenino
F3	1.0	0.76	0.27/0.61	0.56/0.73	0.97/0.81	0.93/0.79	1.2/0.80
F4	0.4	2.4	2.0/2.3	2.6/2.7	1.3±.2/1.3	2.6/2.4	1.7±.5/2.4

[a] Rainfall too scattered on Run F1 for meaningful analysis.

[b] Fraction of average total sampling time during which rain fell.

[c] At apparent plume centerline.

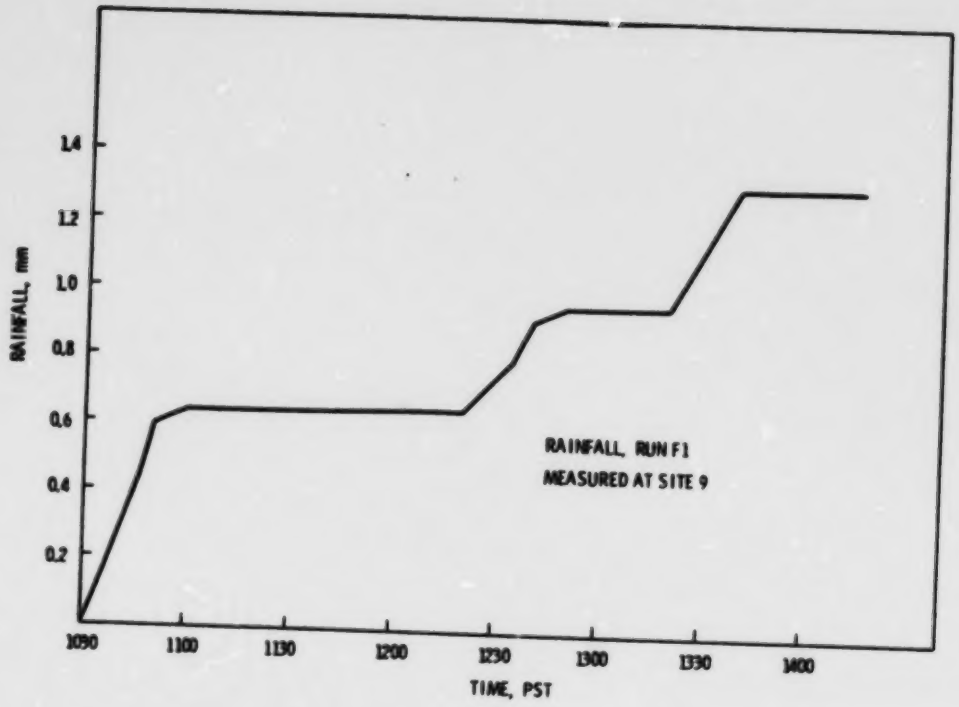

FIGURE 5. RAINFALL AMOUNT VS TIME MEASURED AT THE MOBILE LABORATORY: RUN F1.

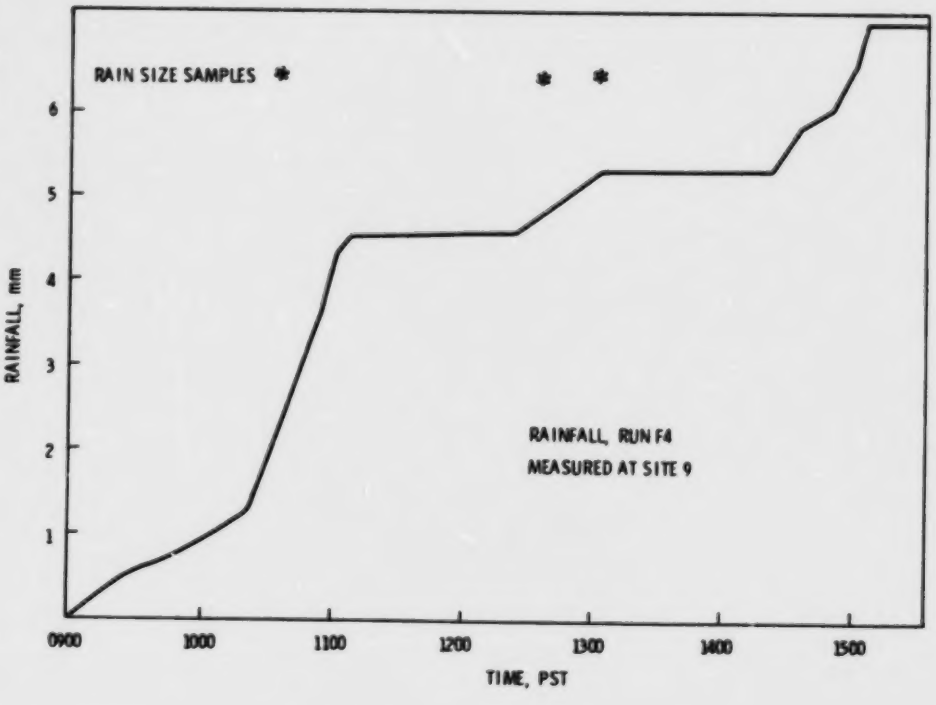

FIGURE 6. SAME AS FIGURE 5, EXCEPT FOR RUN F4.

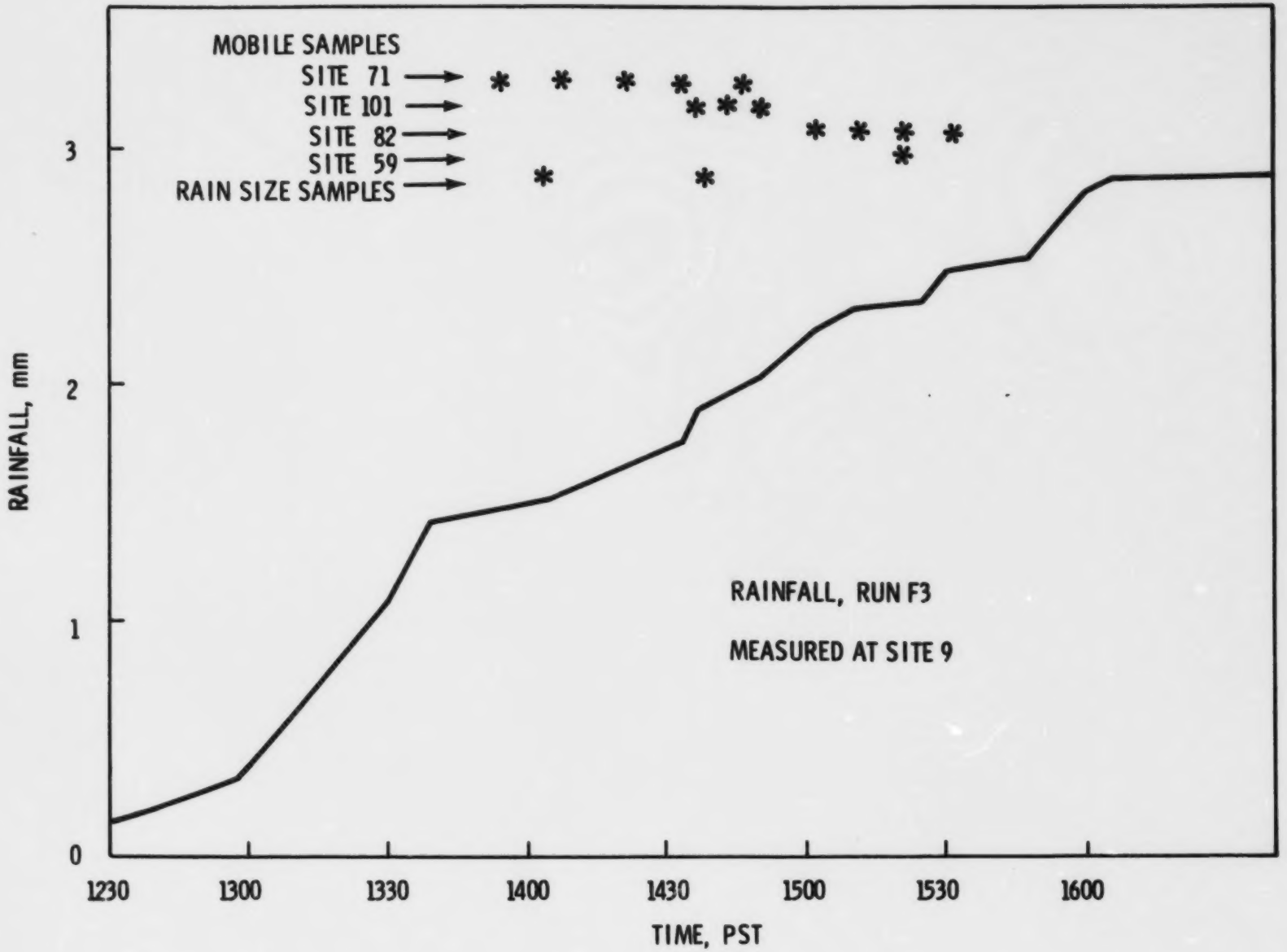

FIGURE 7. RAINFALL AMOUNT VS TIME MEASURED AT THE MOBILE LABORATORY: RUN F3.

(which were largely unobserved with regard to rate and timing) fell elsewhere, both east and west of the apparent plume heading. Comparison of raingauge data with collected rain amounts was then of little value for run F1. The two rainfall rates shown in Table 5 for each site were computed by assuming that the time of rainfall (40% of the total sampling time for F4, and 100% for F3) at the site indicated was the same as that at site 9. The good agreement between the numbers suggests that the rainfall was uniform over the entire array for both runs. Furthermore, in run F4, which contained two or three (depending on the time span of sampler deployment) separate rain periods, it is apparent that the assumption that the rain started and stopped everywhere simultaneously was an acceptable one.

Several raindrop size spectra samples were collected during each of runs F3 and F4. Table 6 lists the spectra chosen from these to represent the rain character of the run as a whole. The choice was made on the basis of a comparison of the rainfall rate from the spectrum to that of the raingauge for the entire run. In F3, the spectra at different times were similar, reflecting the continuous, prefrontal nature of the rainfall. The F4 spectra varied considerably between showers and were more bimodal in character. The chosen spectrum for F4 came from the rain shower which provided the majority of the rain amount to the samples.

Wind and temperature data are listed in Table 7. Run F1 is broken into times roughly coinciding with the rain showers at site 9. The same approach would have been taken for F4, but the data from the plant tower were lost due to instrument malfunction. The only recourse was to visual observations and evidence that the peak SO_2 concentrations in rain occurred at a plume heading of about 180°. The wind speeds during the day (as reported at the Olympia National Weather Service station (17 km north of the plant)) which had that heading were averaged to arrive at an approximate value for the run time of F4.

As is always the case with field experiments of this type, the ideal run is seldom accomplished. This is clear from the overall conditions of the present experiments. The foremost criterion for a successful run is continuous and uniform precipitation over the sampling array; this was met

Table 6. RAINDROP SIZE FREQUENCY[a] DISTRIBUTIONS

Run	Diameter, cm								
	0.022	0.030	0.041	0.055	0.074	0.100	0.140	0.185	0.255
F3	0.005	0.080	0.115	0.100	0.260	0.300	0.135	0.005	
F4	0.040	0.270	0.220	0.130	0.080	0.110	0.080	0.058	0.012

[a] Tabulated values are the fraction of the total number of drops of a diameter less than the diameter listed, and greater than the previous diameter listed.

Table 7. WIND AND TEMPERATURE DATA[a]

Run	Time Span[b]	Speed cm/sec	Direction[c] degrees	Temperature C
F1	1030-1100	580	177	9.5
	1215-1300	380	176±10	10.5
	1315-1345	350	190	10.0
F3	1200-1700	705	174	9.0
F4	1200-1600	∿500[d]	∿180[e]	6.[f]

[a] From 15 minute average data collected at approximate stack top height on plant-operated tower.
[b] Approximate times of rainfall periods.
[c] Azmuth from true north.
[d] Plant tower data missing. Average of hourly speeds from Olympia NWS station which had a direction near 180°.
[e] Visual estimate, and from resulting deposition patterns.
[f] Site 9 surface measurement.

satisfactorily in F3, but the average rainfall rate was low, requiring long sampling times. In addition, the wind speed was generally above average for storms of the region. The strong wind apparently did not seriously affect fixed collector collection efficiencies (see Table 6), but it is undesirable for Line A measurements, since many raindrops collected there undoubtedly undercut the power plant plume. The rainfall of F4 was uniform in extent and timing, but not in rate, and there were dry periods. The latter increases the potential for dry deposition to be a significant component of the concentrations. Run F1 breaks down on several points as a successful run, because the wind direction was probably variable in addition to the rainfall problems noted above.

The times and locations of mobile samples are indicated in Figures 6 and 7. Due to a vehicle breakdown and intermittency of rainfall, none were accomplished during F1. The emphasis was on sequential sampling during F3, once the apparent plume centerline was located. A traverse of the Bucoda area was accomplished at the start of F4 (in place of Central area fixed site deployment) but the eventual letup of rain limited the Central area traverse. Because none of the runs was associated with an extended period of rain, a downwind traverse of mobile sampling (to beyond 11 km downwind) did not occur. After the close of fixed sampling on F4, a series of mobile samples were collected along Line A, during an energetic convective shower. An attempt was made to traverse the plume, but as the shower progressed, the wind direction shifted in the same direction as the traverse. Thus, the samples generally were all taken near or under the plume center. This series of samples did explore the effects of variable rainfall rate and possible changes in concentration with time within an isolated shower.

POLLUTION CONCENTRATIONS IN RAINWATER

The fixed site rain concentrations of the species SO_2, SO_4^{--}, NO_2^-, NO_3^-, NH_4^+, H^+, and PO_4^{3-}, along with rainfall amounts are listed in Tables 17-20 of Appendix A. Similar results, plus rainfall rates, for the mobile samples are listed in Tables 21-23. Where the rainfall amount entry is blank, no sample was collected. Otherwise, blank entries mean that no

analysis was performed. The symbol "NE" indicates that not enough sample was left for analysis for that pollutant. Where a number is preceded by "<", the value is generally the lower detection limit for that pollutant during the analysis session. The symbol "≤" means that the value following is an upper limit, resulting from uncertainty in true concentration due to instrument or calibration problems.

Sulfur Dioxide

On the basis of our experience at Centralia it was clear that the rainfall deposition pattern for SO_2 should be the most discernible. Therefore, for the purpose of locating the plume and identifying samples upon which to emphasize the analyses for other species, we performed the SO_2 analysis first for all samples. The scavenged "plume" of SO_2 is clear in all three runs (though somewhat off the array in F1): Figures 8-10 are maps of the sampling array with numbers representing SO_2 concentration in g-moles/l. The isolines are somewhat schematic in view of the sampling coverage limitations, but represent reasonable confidence regarding the shape of the deposition pattern. Ground-level air concentrations of SO_2, as measured by the bubblers, in parts per billion (1 ppb ≈ 5×10^{-14} g-moles/cm^3) are indicated within the boxes.

A useful indicator of the overall removal rate of SO_2 from a plume is the cross-plume integrated flux or scavenging rate. This quantity, generally the rate of removal per unit time per unit distance downwind, is defined by

$$W = \int_{-\infty}^{+\infty} C(y)\, J\, dy \approx \frac{1}{2} \sum_{i=1}^{n-1} \left(C_i\, J_i + C_{i+1}\, J_{i+1} \right) |y_i - y_{i+1}| \qquad (5)$$

where C_i is the concentration, J_i is the rainfall rate (cm/sec), y_i is the cross-plume coordinate of sample position i, and n is the total number of rain collectors along the cross-plume line. These were calculated from the present data by selecting lines of samplers that crossed the plume, and taking average values of J and y-separation in each case.

FIGURE 8. GROUND-LEVEL RAINWATER CONCENTRATIONS MAP FOR SO_2, RUN F1 (SEE FIGURE 3 FOR IDENTITIES OF SAMPLING SITES).

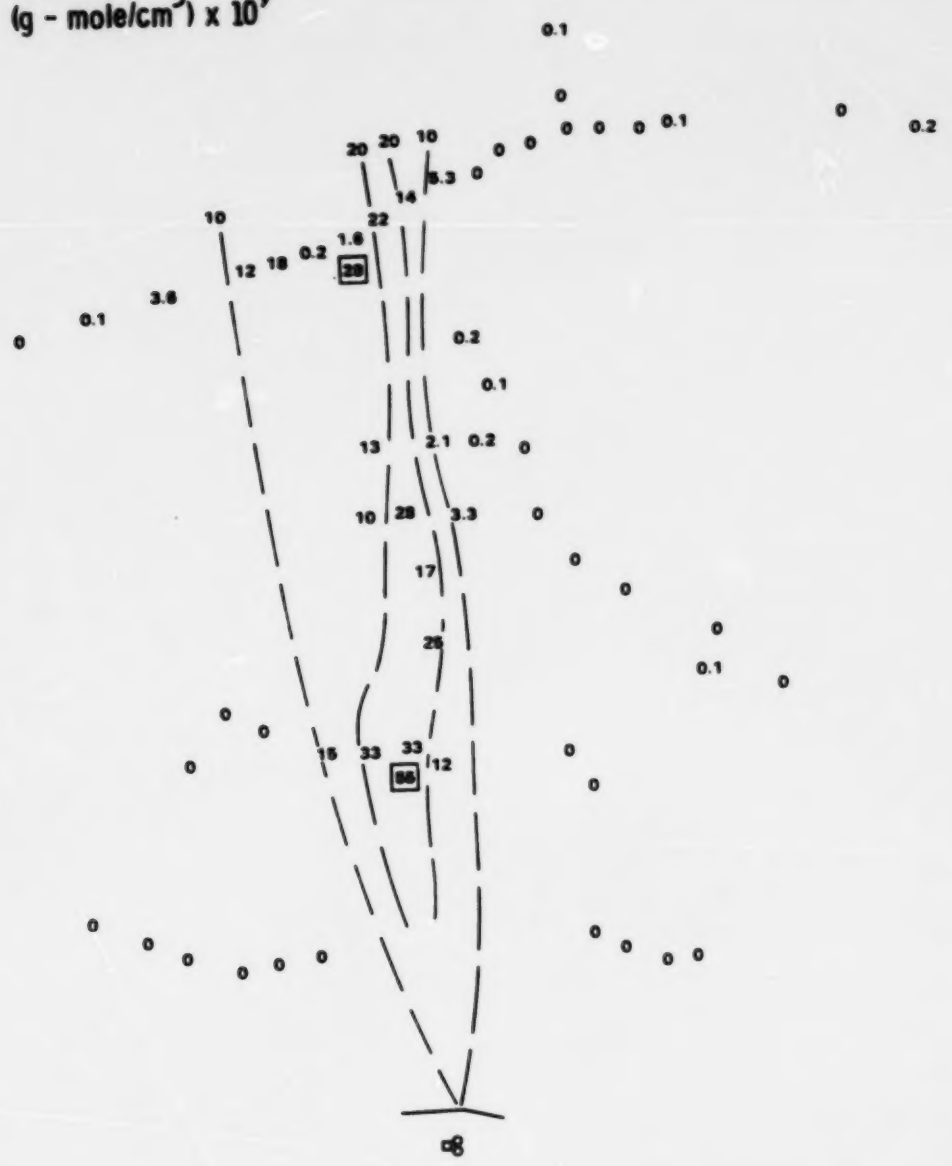

FIGURE 9. SAME AS FIGURE 8, EXCEPT FOR RUN F3. BOXES SHOW AIR CONCENTRATIONS IN ppb.

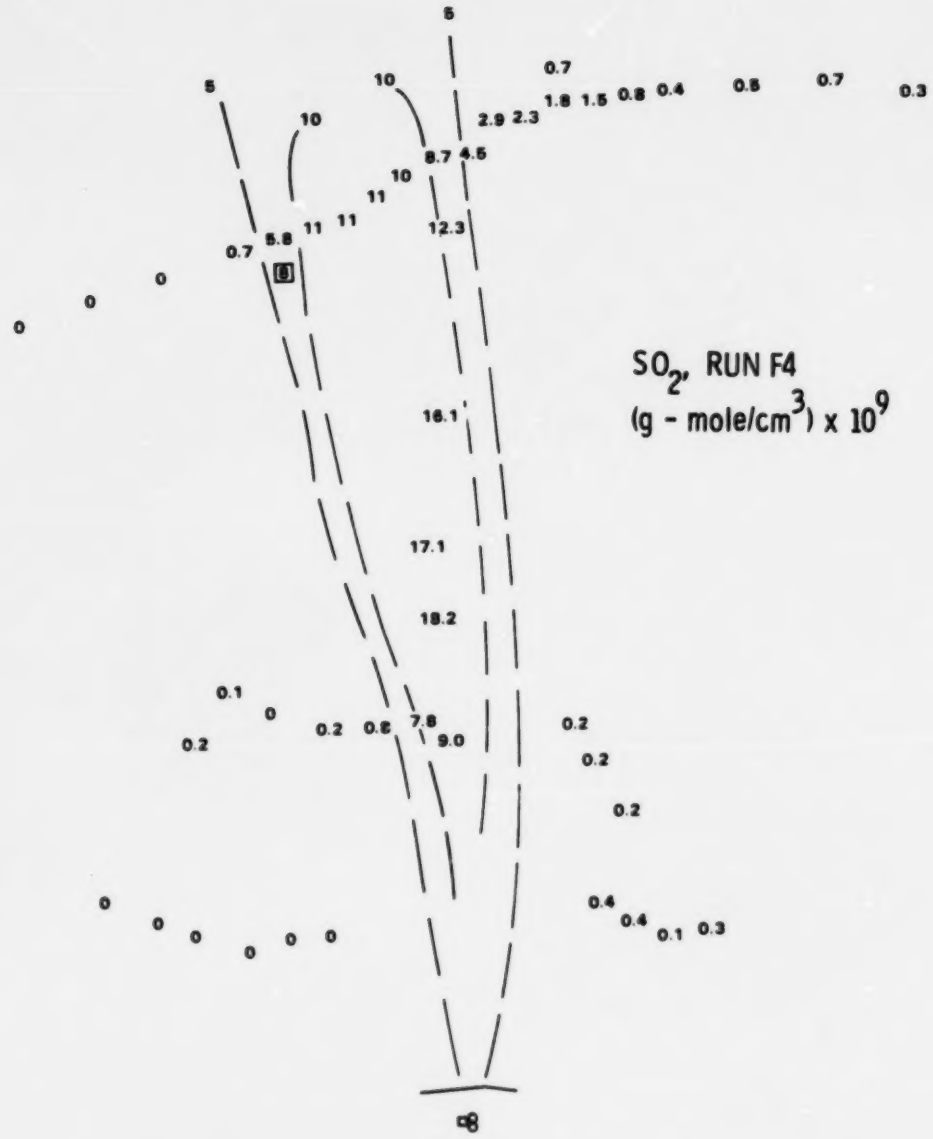

FIGURE 10. SAME AS FIGURE 8, EXCEPT FOR RUN F4. BOXES SHOW AIR CONCENTRATIONS IN ppb.

The results are listed in Table 8 and plotted as a function of downwind distance x in Figure 11. For comparison, the results of previous similar experiments[3,12] are shown in the graph. Relevant source and meteorological conditions are listed in Table 9. The great variability in scavenging rates for SO_2 at the nearest distance has been discussed before in connection with the "C" series runs[3]. In brief, this variability results mainly from undercutting of the plume by small raindrops and near miss of the SO_2 source by other raindrops. In the former case, very low concentrations will result if a significant amount of the mass of rain is in sufficiently small drops. In the latter case, the reversible scavenging behavior of SO_2, being sensitive to sharp changes in air concentration and rain acidity, can potentially result in a wide variety of rain concentrations to the ground. The tendencies for sampler-surface desorption may be sharply variable as well - this is a function of plume characteristics. All these factors are dependent on the mean wind speed, and the wind shear, as well as on the character of the rain size spectrum. These are all difficult to measure and characterize as an average for the 1 1/2 to five hour sampling times.

The bunching of the scavenging rates within a reasonably narrow range at $x \geq 2.5$ km is probably the result of the tendency for the power plant plume to assume a similar character whenever rain is falling. This reflects the fact that SO_2 scavenging is essentially "equilibrium scavenging": the ground-level rain concentrations of SO_2 are those which are in equilibrium with the ground-level air concentration of SO_2. The scavenging rates then reflect the nature of the SO_2 plume at ground level. These essentially equilibrium scavenging rates become slightly more bunched if one "normalizes" them in terms of Q/u (to which the air concentration is proportional), and J. Some of the remaining variability would result from experimental error (discrete concentration measurements) and topographic effects, which might tend to misshape the plume when the mean plume heading varies slightly.

Sulfate

The analysis for sulfate ran concurrently with that for SO_2. Because of an apparent laboratory contamination problem associated with the F1 samples, and

Table 8. SCAVENGING RATES FOR SO_2: COMPARISON OF PRESENT RESULTS WITH THOSE OF THE PREVIOUS STUDIES

Experiment	Reference	Scavenging Rate at Distance x Downwind[a] (gram-moles/cm sec) x 10^9				
		0.4-0.5 km	2.4-3.4 km	4.5 km	7.0 km	10-11.5 km
C-2	3	26.	86.	b	b	66.
C-3	3	0.14	33.	b	b	83.
C-4	3	b	98.	b	136.	233.
C-5	3	1.1	b	b	b	21.
C-A	12	45.	b	b	b	b
F3	Present	3.0	b	100.	54.	115.
F4	Present	27.	b	42.	b	129.

[a] Range of distances downwind reflect differences in mean line distances due to different sampling arrays and mean plume headings.

[b] Insufficient measurements.

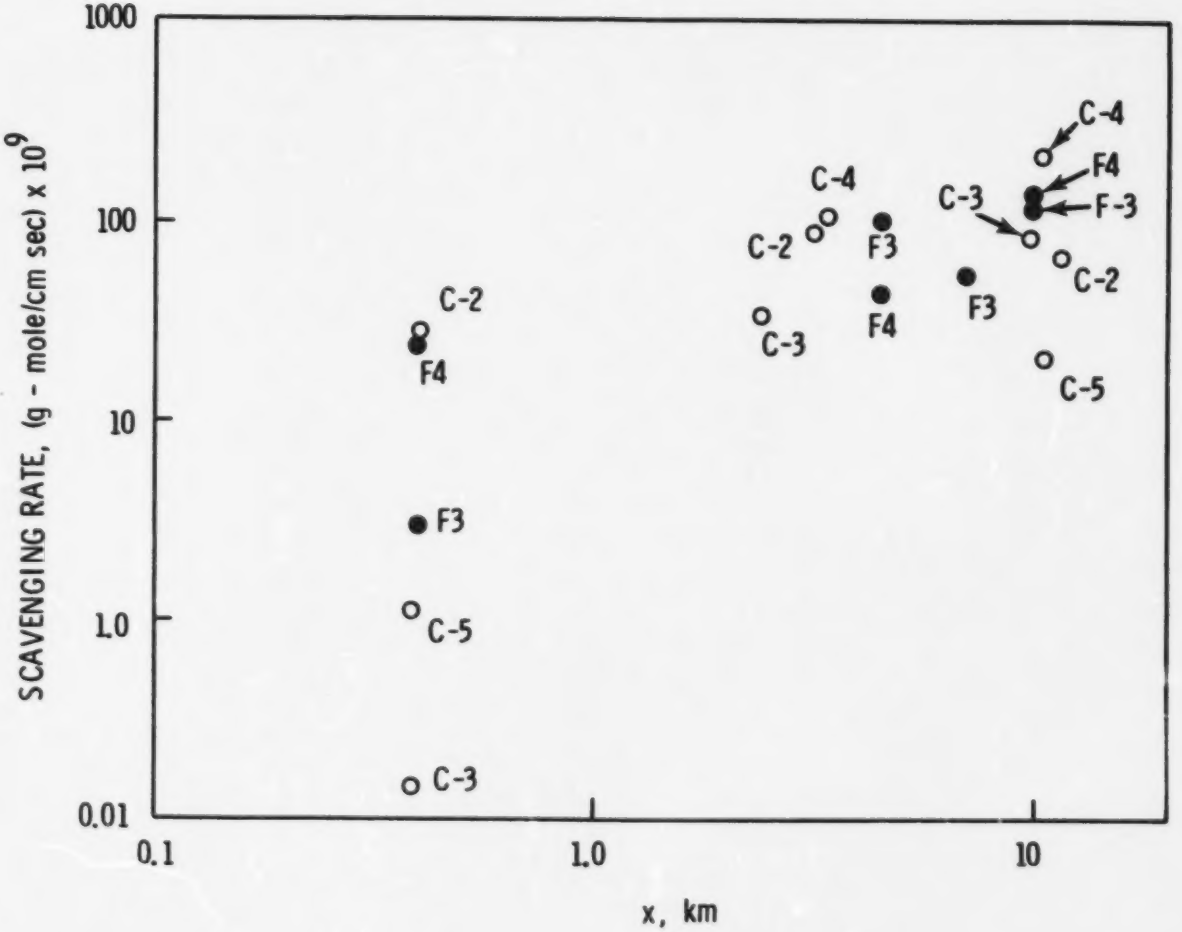

FIGURE 11. MEASURED SCAVENGING RATES FOR SO_2 (cf.(5)) AS A FUNCTION OF DOWNWIND DISTANCE x.

Table 9. METEOROLOGICAL AND SOURCE CONDITIONS RELEVANT TO SCAVENGING RATE COMPARISONS

Run	Date	J[a] mm/hr	Wind Speed cm/sec	Sulfur Source Strength gram-moles/sec	Background Rain pH
F3	12-10-74	0.8	705	25.4	5.3
F4	12-12-74	2.4	500[b]	25.7	5.4
C-2	2-28-72	3.5	541	9.3	5.7
C-3	3-1-72	0.8	547	13.5	6.1
C-4	3-5-72	2.3	800	16.1	5.4
C-5	3-9-72	1.3	345	11.7	4.7
C-A	3-1-74	3.0	141	9.8	4.8

[a] Average at raingauge site.

[b] Estimate - see Table 7.

instrument difficulties during the F3 sample analysis sessions, a complete examination of sulfate concentrations was not accomplished on the first analysis "pass." A selection of F3 and F4 samples were then rerun for sulfate. Sulfur dioxide tends to oxidize to sulfate in bulk (unfrozen) water samples*; it was necessary then to reexamine the SO_2 concentration to assess the extent of conversion of previously measured SO_2. The sulfate concentration is then determined by subtracting the (molar) concentration of converted SO_2 from the total (molar) sulfate concentration. Often conversion was substantial, so that the resulting sulfate concentration determined for the sample was the difference between two rather large numbers. The error resulting from this process then effectively cut accuracy such that values for sulfate concentration listed in the tables whose magnitudes are below about 10 micromoles/l are uncertain by at least 50%. In general the sulfate molar concentrations were not large compared with those of SO_2, so that it was difficult to define a deposition plume for sulfate. This fact is shown in the sulfate concentration maps, Figures 12-13, where the only discernible plume-related sulfate deposition appears at downwind distances greater than about 7 km.

Hydrogen Ion

The hydrogen ion deposition patterns in Figures 14-15 generally reflect the presence of the power plant plume (as defined by the SO_2 deposition pattern). Among the species whose concentrations were determined, sulfate is the only apparent significant contributor to rain acidity above the background level. Comparisons between the H^+ and SO_4^{--} concentrations for runs F3 and F4 show considerable scatter; whereas $H^+ = 2SO_4^{--}$ would suggest that the acidity is due to sulfate in the absence of other ionic species. A good deal of this scatter could be accounted for in terms of inaccuracies in measuring sulfate, as noted above; in addition, there may be other species in the rain, not measured, which could contribute to the acidity. Local sources of effective materials at certain sites may have influenced some of the data. Of

*Samples were normally unfrozen for up to 8 hours during each analysis session. They were refrozen, however, between analysis sessions.

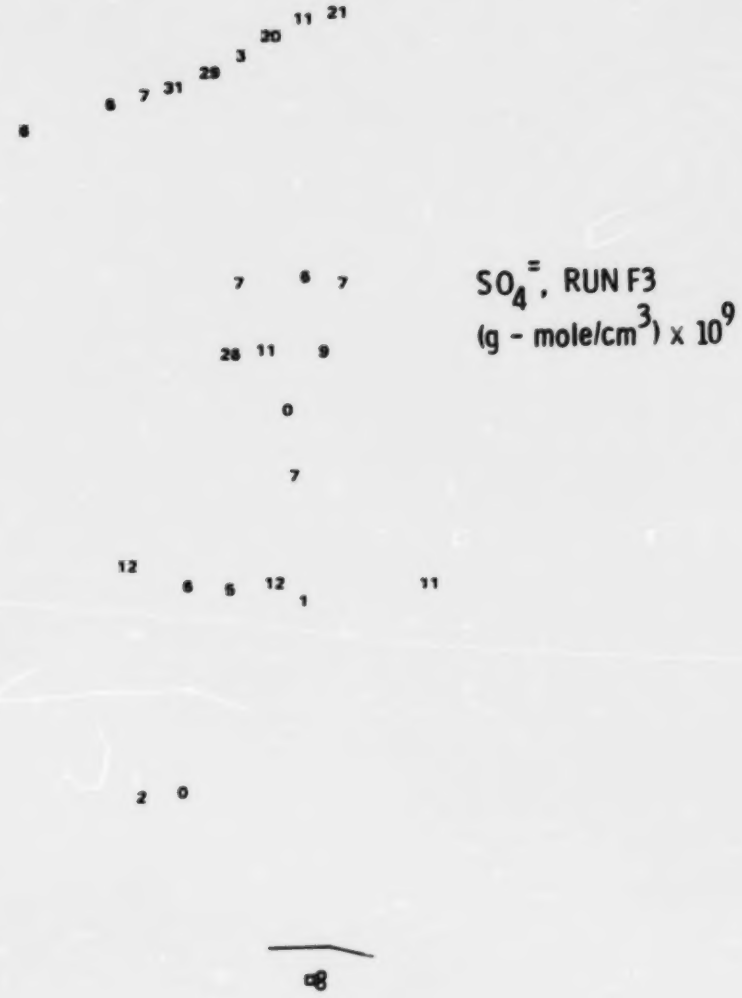

FIGURE 12. GROUND-LEVEL RAINWATER CONCENTRATIONS MAP FOR SULFATE. RUN F3. SEE FIGURE 3 FOR IDENTITIES OF SAMPLING SITES.

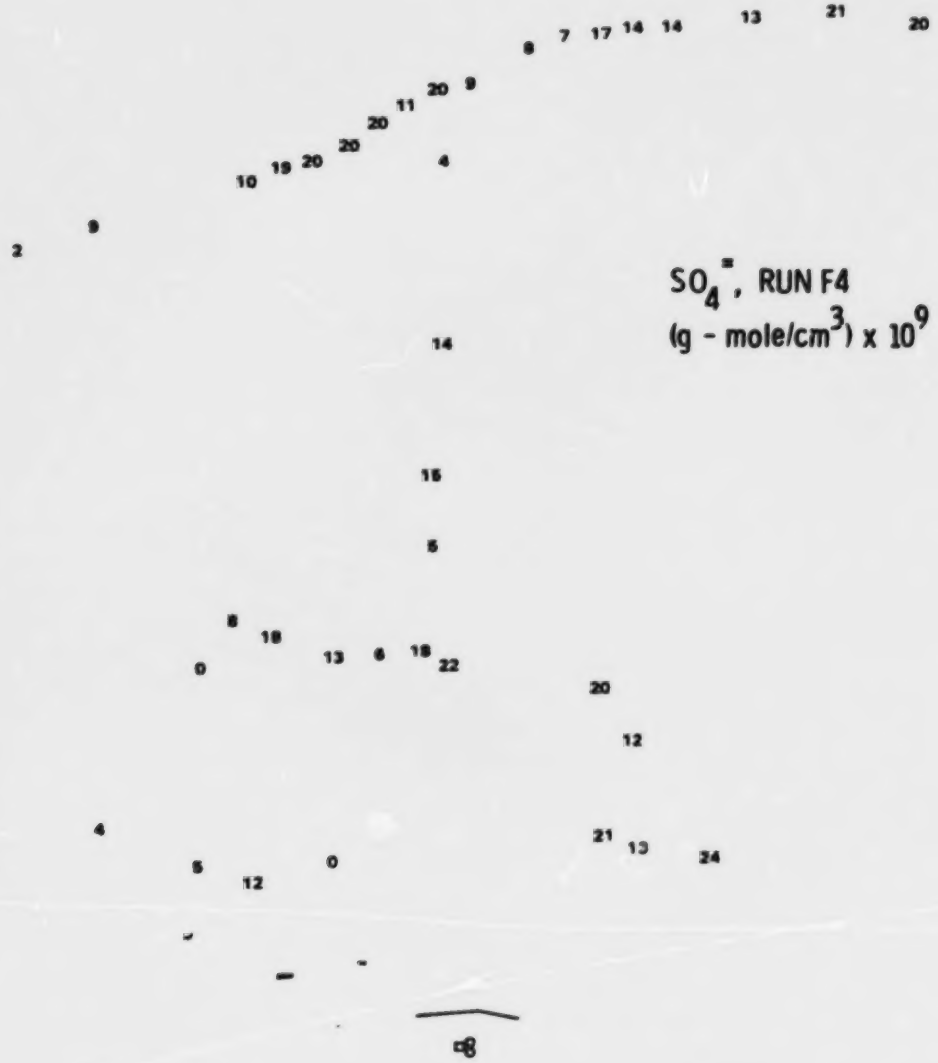

FIGURE 13. SAME AS FIGURE 12, EXCEPT FOR RUN F4.

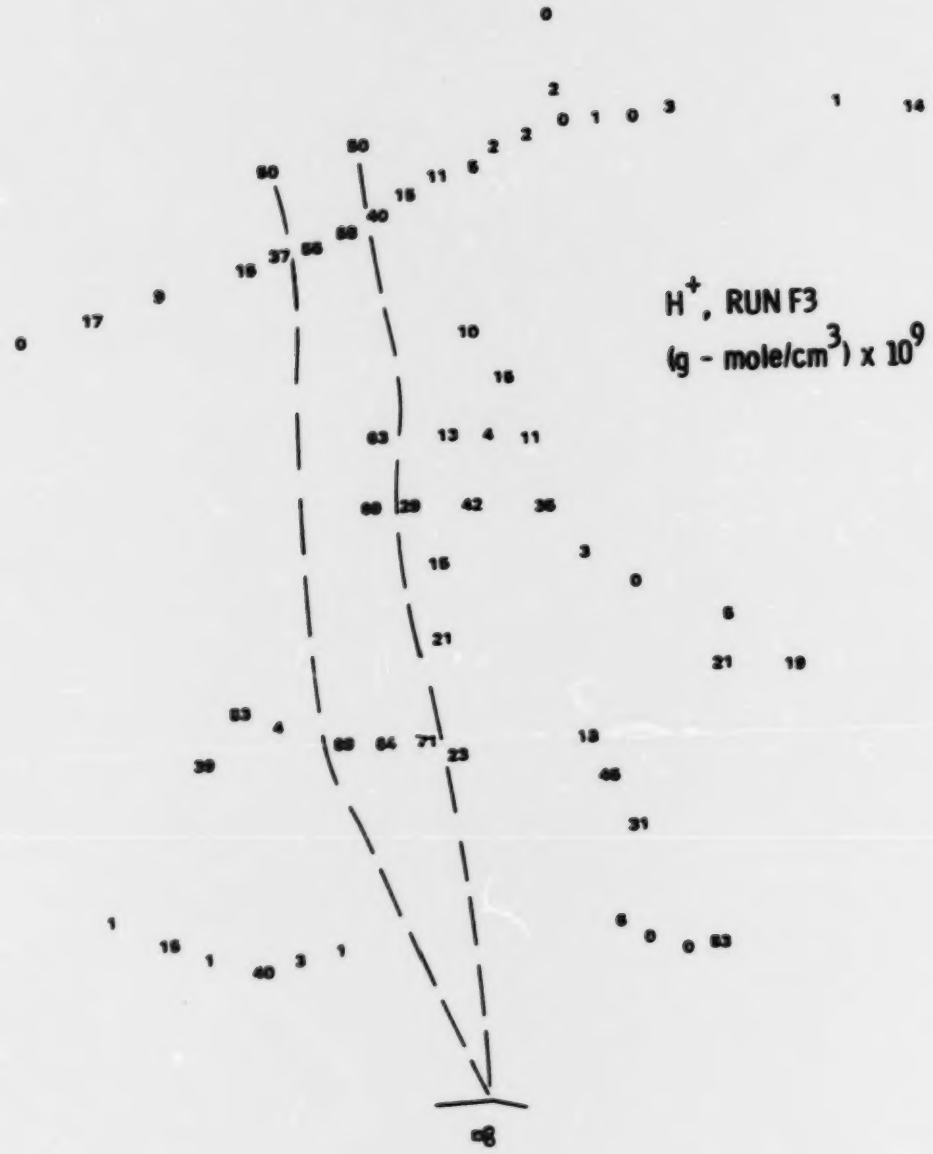

FIGURE 14. GROUND LEVEL RAINWATER CONCENTRATIONS MAP FOR H^+, RUN F3.

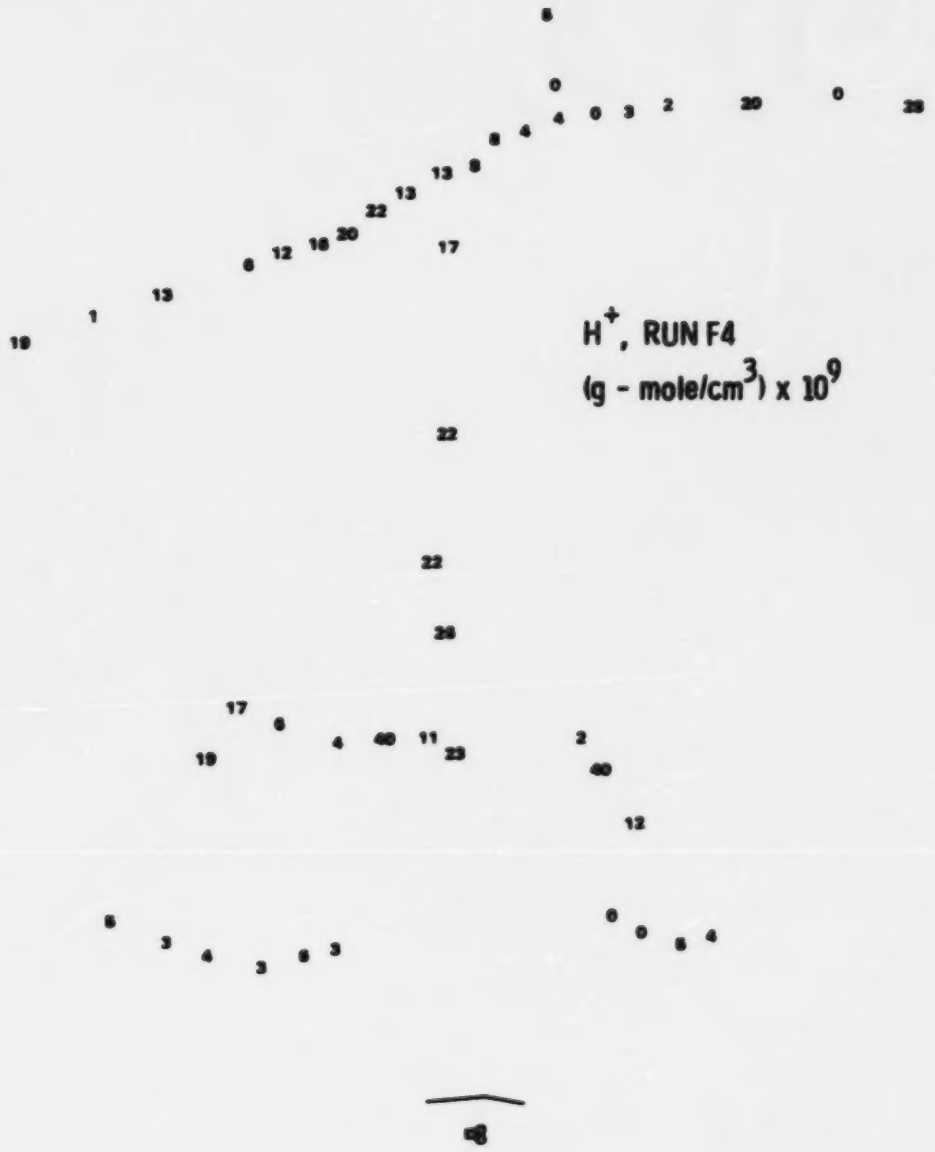

FIGURE 15. SAME AS FIGURE 14, EXCEPT FOR RUN F4.

particular interest in this regard, however, is the H^+-SO_4^{--} relationship for the line of sampling sites in the Tenino area, at a distance of about 10 km downwind. These data, for Run F3, are shown in Figure 16.

The balance between $H^+/2$ and SO_4^{--} concentrations is quite good in this area, except at two sites, presumably in the center of the plume, where the SO_2 concentrations appeared very low. It is true that "negative washout" of SO_2 can occur where the rain acidity is so high that SO_2 solubility is significantly reduced[3]. From all available data for this run, however, this does not appear to be the case, inasmuch as the H^+ concentration at these points was not sharply larger than at other sites where significant SO_2 appeared. For example, the same sites in Run F4 provided a quite continuous broad flat peak in the concentrations of SO_2, sulfate, and H^+. In this case, the H^+ concentration was less than half of the sulfate concentration, as it appeared to be for most of the other sites for that run.

Nitrogen Compounds and Phosphate

There appeared to be no power plant plume-related trend to the measured rain concentrations of NO_2^-, NH_4^+, NO_3^-, and PO_4^{3-}. The concentrations ranged from near detection limits to values which are not excessive in comparison with levels observed in unpolluted areas[18-24]. There were some sites which consistently showed significant concentrations, however. In the case of nitrite, these sites were generally those located near a railroad or highway. The rain in some farming areas, particularly at sites near active cattle pastures and corrals, contained elevated ammonium ion concentrations. One *group* of sites showed high NH_4^+ concentrations during run F4. This cannot be explained in terms of power plant effects or agricultural sources; it is conceivable that some contamination was present in the area operator's vehicle or some source of contamination traversed the road along which the samples were collected.

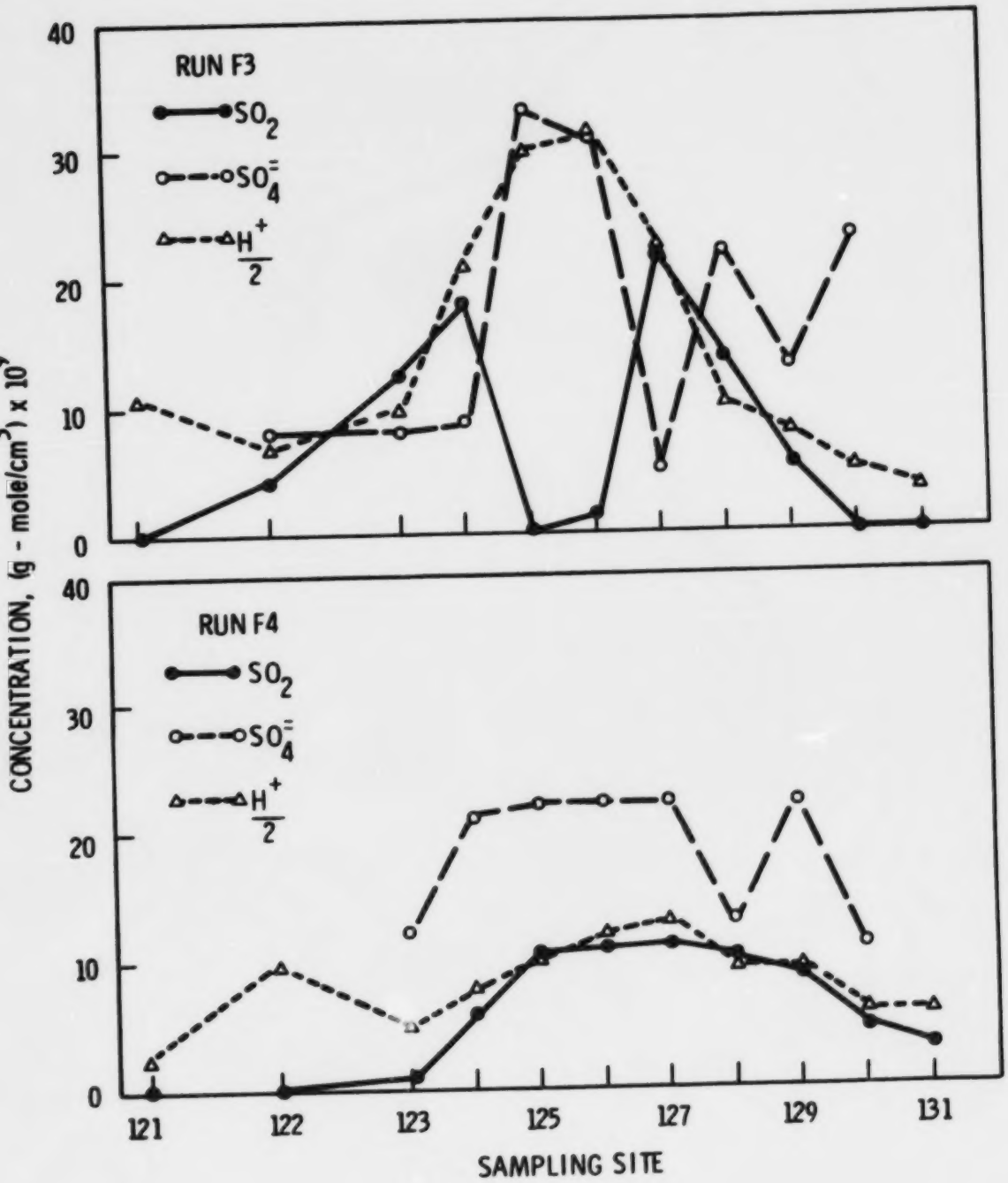

FIGURE 16. CROSS-PLUME RAINWATER CONCENTRATIONS PROFILES IN TENINO AREA (x ~10 km).

AIR CONCENTRATIONS

Table 10 lists the air concentrations measured by the bubbler/impinger methods for NH_3 and O_3. Concentrations of the bubbler solutions for NH_3 were determined in the same manner as the rain samples, the solutions having been acidified to form NH_4^+. The O_3 concentrations were determined by manual means in the field, on the same day as collection. The lower concentrations, in the region of 1 ppb, are approximate, due to doubts about the validity of the bubbler technique for measuring very low concentrations[25]. Other error indications are the result of uncertainties in bubbler solution volume flow rates, and actual time of sampling due to bubbler malfunction. SO_2 air concentrations are indicated on the SO_2 deposition maps, Figures 8-10 and in Table 11.

INSOLUBLE PARTICLE ANALYSES

Several fine pored membrane filters (0.1 micron Millipore) were exposed to falling raindrops at the same time as mobile rain samples were collected. These were expected to represent the rain falling through the central portion of the power plant plume, as indicated by pH measurements on the scene and, later, the SO_2 concentration in the rain samples. The filters were exposed so that raindrop spots on the filters would not overlap; thus, the images of particle-containing drops were expected to be visible on the filter when later examined by electron microscopy. Such examination was conducted for several of the filters, but it was found that the images were not readily apparent. In addition, there were insufficient numbers of particles on the filters to make extensive scanning electron microscope (SEM) with X-ray fluorescence analysis practical. It was then decided to effectively concentrate the particles from the rain on filter surfaces by filtering the bulk rain samples, using the same filter material. This increased the surface density of particles by about a factor of one hundred (considering the volumes of rain samples on hand), but, of course, individual raindrop images were not obtained.

Table 10. MEASURED AIR CONCENTRATIONS OF NH_3 AND O_3

Run	Site	O_3 Time of Sample, min	O_3 Volume of Air Sample ℓ	O_3 Concentration ppb	NH_3 Time of Sample, min	NH_3 Volume of Air Sample ℓ	NH_3 Concentration ppb
F1	BKG	412	490	3.9	412	535	3.5
F2	BKG	357	480	14.5[a]	357	430	≤1.
	8	186	240	135.[a]	b	b	b
	11	182	260	4.2[a]	b	b	b
F3	BKG	271	310	8.3	271	310	1.7
F4	BKG	261	300	11.4	261	300	≤1.
	7	162	185	5.2	b	b	b
F5	BKG	350	400	17.3	350	400	≤1.
	8	241	275	2.9	b	b	b
	71	b	b	b	258	530	≤1.

[a] May be contaminated by previously used impinger.

[b] No measurement.

Table 11. MEASURED AIR CONCENTRATIONS OF SO_2

Run	Site[a]	Time of Sample, min	Volume of Air Samples ℓ	Air Concentration[b] (gram-moles/cm^3) x 10^{12}	ppb[c]
F1	BKG	412	490	<.04	<1
	8	246	340	<.04	<1
	9	250	360	<.04	<1
	10	259	360	<.04	<1
	11	264	375	<.04	<1
	71	349	385	<.04	<1
F2[d]	8	186	260	<.04	<1
	10	184	270	<.04	<1
	11	182	240	<.04	<1
	71	216	320	0.71	16.
	84	330	300	0.28	6.3
F3	BKG	271	310	<.04	<1
	6	155	175	0.05	1.7
	10	49	55[e]	0.25	5.6
	71	182	250	2.3	55.
	126	184	250	1.2	28.
F4	BKG	261	300	<.04	<1
	5	161	185	<.04	<1
	10	222	255	<.04	<1
	71	198	190	<.04	<1
	74	171	195	.04	1.0
	124	203	260	0.52	12.
F5	BKG	350	400[f]	<.04	<1
	6	245	280	<.04	<1
	8	245	275	<.04	<1
	59	258	550	.08	1.8

[a] See Figure 3. BKG 4.3 km upwind of power plant.
[b] Lower limit for bubbler/impinger method arbitrarily chosen as 1 ppb.
[c] Based on Run temperature (Table 7) and a pressure of 1 atm.
[d] Non-precipitation run.
[e] Represents only a small portion of the total run time.
[f] Bubbler flow rate not measured; estimated as same as others.

Four of the mobile rain samples were so treated, and the filters examined by SEM. (One of the fixed-site samples -- exposed for several hours rather than several minutes -- was also filtered and examined, but the particle content, presumably from local sources, was very high. Apparently, fixed-site containers will accumulate quantities of organic matter or other debris, which does not seem to affect the inorganic, nonmetallic pollutant analyses, but does lead to large insoluble particle counts.) Table 12 lists the samples treated and some rough estimates of the count of particles per cm^3 of rain. These order-of-magnitude estimates are based on counts of particles residing on small, known filter areas and known filtered rain amounts. Sample 66A (run F4; see Table 22) is considered to be a background sample as far as the power plant plume is concerned, because of its relatively high pH (5.19) and low SO_2 concentration (1.0×10^{-9} g-moles/cm^3). The particle density on the filter was about one hundredth that of the samples collected under the plume.

A large fraction of the particles appearing on the under-plume filters were spherical or very nearly spherical in shape. These particles are assumed to be products of an efficient, high-temperature combustion process[26]. The numbers present indicate that the source is probably the power plant. Such particles were observed on filter 66A, but in very much fewer numbers. Examples of the particles observed on two of the filters are shown in Figures 17 and 18.

The chemical composition of several of the particles on each filter was examined by X-ray fluorescence techniques, using the primary electron beam of the microscope to promote X-rays whose energies could be characterized in terms of the elements present. The most abundant element among those analyzable by this method (generally of molecular weight above that of Na) was usually Si, though some angular particles were primarily iron. The spherical particles had X-ray spectra which were more alike than those of the angular particles (some of the latter of which were sand; i.e., nearly all Si), with a primary emission peak corresponding to Si, secondary Al, and small peaks representing Ca, Fe, K, and Ti. The non-spherical particles were generally more diverse in content, with S, Zn, Ce, K, Zr, Mg also

Table 12. RESULTS OF ELECTRON MICROSCOPE ANALYSES OF FILTERED RAIN SAMPLES

Run	Sample[a]	Volume[b] mℓ	Volume of Water in Count Sample[c] mℓ	Estimated Particle Concentration[d] cm^{-3}	
				Total	Spherical
F3	71B	133	7.1×10^{-4}	50,000	5,000
F3	82C	66	3.9×10^{-3}	20,000	5,000
F4	66A	78	0.042	500	0

[a] See Tables 21 and 22 for soluble pollutant concentrations.

[b] Remaining after soluble pollutant analyses.

[c] Volume of water from which count was made = total volume X $\frac{\text{area of microscope photograph}}{\text{total area of filter } (17.35\ cm^2)} \times \frac{1}{\text{Magnification}}$.

[d] Particles diameter $\gtrsim 1\mu$; Order-of-magnitude estimate.

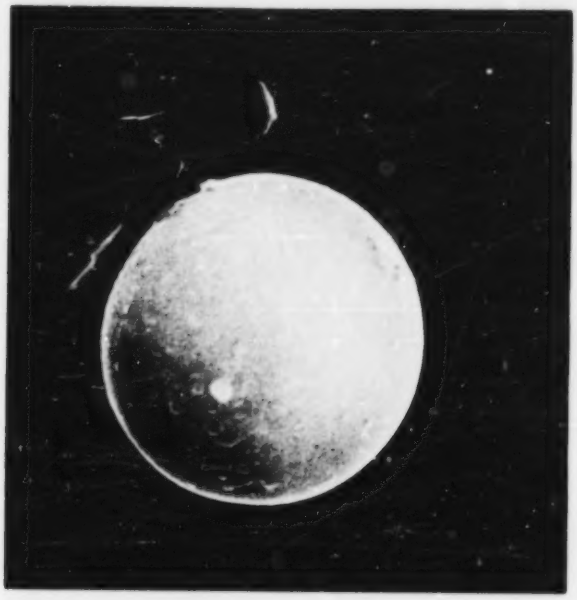

FIGURE 17. SCANNING ELECTRON PHOTOMICROGRAPH OF A PARTICLE FROM MOBILE RAIN SAMPLE 71 B. THE DIAMETER IS ABOUT 4.9 µm.

FIGURE 18. SCANNING ELECTRON PHOTOMICROGRAPH OF PARTICLES FROM MOBILE RAIN SAMPLE 82 C. THE DIAMETER OF THE SPHERICAL PARTICLE IN RIGHT CENTER IS ABOUT 5.5 µm.

appearing, but had much less Al than the spherical particles. Some of the angular particles showed more X-ray "hash" of low energy which corresponds often to a significant amount of carbonaceous or organic materials.

Despite the concentrating effect that the bulk filtration had on the individual particle analyzability, the volumes of water associated with the mobile samples were still too small to provide a sufficiently densely coated filter for practical particle sizing and determination of particle size distributions. This would be possible, given the same conditions as were extant during the present experiments, with the filtration of about 1 liter of water. A good deal of the funds budgeted for the SEM work was used in the unsuccessful examination of the rain-spot filters. Future work with bulk rain sampling should give promising results, particularly in relating the fly ash particle counts and masses with other pollutant concentrations, and in determining the particle size distribution of scavenged insoluble particles. An interesting comparison can possibly then be made with the particle size spectrum which escapes the precipitators; the results could reveal much about the scavenging efficiencies of various-sized fossil-fuel effluent particles.

SECTION VII.

COMPARISON OF SMICK CALCULATIONS WITH OBSERVED DATA

The Scavenging Model Incorporating Chemical Kinetics was applied to input conditions corresponding to the major experiments of the two Centralia field series. The sulfur dioxide oxidation mechanism employed in the calculations was the liquid-phase ammonia-involved model of Scott and Hobbs[10]. Whereas these authors considered the liquid phase in the atmosphere in general, constant atmospheric concentrations of SO_2, NH_3, and CO_2, and fixed values of the equilibrium constants for the dissolution of these gases, the present treatment assumes that SO_2 is scavenged reversibly from a specified plume to raindrops which are distributed in size. The reactions involved in the Scott and Hobbs mechanism (described in Appendix B) are included in the concentration calculations, performed at various levels (as required by the SO_2 scavenging regime) along the raindrops' trajectories. The result is a test of the ammonia model's ability to account for the observed values of rain concentration of sulfate at ground level.

It should be noted that some assumptions have been made, in lieu of more precise knowledge of some of the contributing factors. Perhaps the most important of these is the inclusion of a constant value for ammonia gas-phase concentration and solubility constants. The latter value is based on measurements made at high gas-phase concentrations only[27]. In addition, the equilibrium constants used in the intermediate reactions (involving NH_3, NH_4^+, CO_2, HCO_3^-, CO_3^{--}, and H^+) are taken as constants, and at values listed in the literature for a temperature of 25 C. Moreover, there is considerable dispute about the magnitude of the assumed first order rate constant K for the final step, the oxidation of SO_3^{--} to SO_4^{--}. Various treatments of the laboratory data have led to a range of values for this constant. We have considered two values for K which differ by an order of magnitude; these correspond to that suggested by Scott and Hobbs, and to a value given later by McKay. Appendix B contains a listing of equilibrium constants and the reactions involved.

Preliminary to the application of SMICK to a plume situation, several calculations were performed assuming a constant value for the gas-phase concentrations of SO_2. The results, listed in Table 13, correspond with the calculations performed by Scott and Hobbs[10], but in this case, the liquid phase consists of raindrops distributed in size, and the solubility of SO_2 is dependent on gas-phases mixing ratio y_{SO_2}. Since y_{SO_2} is held constant, the liquid phase concentration is in equilibrium with the gas phase, and is also constant for all drop sizes. These calculations were performed for the smaller values of K = 0.0017 sec^{-1} only. (As will be shown below, an increased K will result in predicted increases in the sulfate concentrations, but not significantly those of SO_2, NH_4^+, or H^+.) It should be noted that the concentrations reported as "SO_2" (both observed and calculated) in this report are the sum of the concentrations of aqueous-phase SO_2, HSO_3^-, and SO_3^{--}. This is necessitated by the measurement technique for dissolved SO_2, which determines all three species. The magnitude of the concentration of HSO_3^- generally predominates the others, the first dissociation process being nearly complete under most circumstances[4].

Table 13. SMICK CALCULATIONS WITH SCOTT AND HOBBS[10] MECHANISM: UNIFORM GAS PHASE SO_2 CONCENTRATION.

Gas phase concentration, ppm			K, sec^{-1}	Concentration, (gram moles/cm^3) x 10^9			
NH_3	CO_2	SO_2		SO_2[a]	$SO_4^=$	NH_4^+	H^+
5	311	5	0.0017	1.9×10^5	1.0×10^4	2.3×10^5	0.47
0.007	311	0.007	0.0017	260	13.9	332	0.47
0	311	0.007	0.0017	10.2	0.03	0	10.7
0	311	5	0.0017	287	0.03	0	282

[a]See note a, Table 14.

The wide range of concentrations resulting from variations in y_{NH_3} and y_{SO_2} illustrates the strong influence of ammonia predicted by this model. The third case listed -- the Scott and Hobbs case for the general atmosphere -- presents the most realistic results in terms of a non-plume precipitation situation. Clearly, the presence of ammonia is required in this mechanism for any significant sulfate to appear, but the process also leads to rather large ammonium ion concentrations and high pH.

The SMICK calculations, employing the Scott and Hobbs[10] mechanism, a bivariate-normal plume and actual experimental input data, are listed in Table 14. Each concentration is a plume centerline value which is the bulk rain concentration, averaged for rain size spectra measured during the runs. Relevant input data for the current experiment series ("F" runs) are listed in Tables 3-9; input data for the earlier "C" runs are listed in Table 9 and in another report[3]. For comparison are given the observed peak concentrations at the various downwind distances, and the results of calculations employing the EPAEC-mode of SMICK (SO_2 scavenging only). The latter calculation involves no decay function for the SO_2 in the plume (no conversion or prior scavenging is considered); thus, the results may be better compared with the sum on the observed SO_2 and sulfate concentrations, rather than with the observed SO_2 concentrations alone. The value of K used for Table 14 calculations is that measured by Van den Heuval and Mason[28]. Two values of y_{NH_3} were used: 7 ppb, as used by Scott and Hobbs, and considered to be a reasonable background level[29,30]; and 1 ppb, perhaps a more realistic one for the Centralia area (as indicated by measurements, see Table 10). All the calculations employed the Smith and Singer[31] values of the plume standard deviations; the centerline values are comparable, but may not necessarily reflect the real plume situation, there being room for considerable variation in plume centerline concentrations if the parameters are changed slightly.

In the case of either value of y_{NH_3}, the predicted NH_4^+ content and pH are significantly higher than any measured. This follows as a direct result of the reactions included in the mechanism. The large predicted concentrations of dissolved SO_2 result directly from the increased alkalinity, inasmuch as the solubility of SO_2 is a strong decreasing function of excess H^+ concentration. The latter is calculated at each vertical calculation

Table 14. CALCULATED PLUME CENTERLINE RAINWATER CONCENTRATIONS: SMICK (SCOTT AND HOBBS; K = 0.0017 sec^{-1}) AND EPAEC (SO_2 ONLY).

		Concentration, (gram moles/cm^3) x 10^9								
		PNH_3 = 1 ppb (7 ppb)					Observed[b]			
Run	x km	SO_2[a]	$SO_4^=$	NH_4^+	H^+	SO_2 (EPAEC)[c]	SO_2[a]	$SO_4^=$	NH_4^+	H^+
C-2	3.1	273 (350)	1.3 (6.2)	287 (438)	2.5 (0.6)	64.	11.0	30.	d	20
	11.5	86 (107)	2.4 (9.0)	105 (191)	1.0 (0.3)	24.	4.0	16.	d	8
C-3	2.4	924 (1950)	2.3 (14)	932 (2060)	10. (2.5)	102.	23.0	d	d	50
	10.9	278 (545)	6.1 (31)	300 (680)	3.2 (0.8)	36.	13.0	d	d	32
C-4	3.5	407 (640)	1.7 (8.8)	419 (736)	4.0 (1.0)	60.	15.0	52.	d	50
	7.0	223 (340)	2.5 (12)	239 (438)	2.5 (0.5)	35.	12.0	20.	d	32
	11.2	147 (225)	3.3 (15)	166 (324)	1.6 (0.4)	23.	12.0	15.	d	25
C-5	11.2	183 (298)	4.1 (19)	203 (406)	2.0 (0.5)	23.	6.2	9.4	d	~30
F-3	4.5	519 (841)	2.2 (11)	531 (944)	5.0 (1.3)	68.	33.	14.	2.4	79
	7.0	356 (564)	2.9 (14)	371 (669)	4.0 (0.8)	47.	28.	28.	3.6	79
	11.2	256 (403)	3.6 (17)	274 (511)	2.5 (0.6)	34.	22.[e]	33.	2.5	63
F-4	4.3	485 (710)	1.9 (9.4)	497 (807)	5.0 (1.0)	92.	9.0	24.	19.5	32
	7.0	321 (460)	2.4 (11)	336 (558)	3.2 (0.6)	63.	18.	17.	5.0	32
	10.2	232 (331)	3.0 (14)	249 (430)	2.5 (0.5)	47.	11.	22.	6.5	32

[a] $(SO_2)_{aq} + HSO_3^- + SO_3^=$

[b] The peak values of all the species are not necessarily recorded at the same sampling site.

[c] No decay of SO_2 with travel time (compare with observed $SO_2 + SO_4^=$).

[d] No measurement.

[e] "Centerline" value was anomalously low. See Figure 16.

step as are all the other relevant concentrations. The predicted values for sulfate concentration are of the same order of magnitude as those observed, but clearly the means by which they are arrived at (including high NH_4^+ and low H^+ values) are inappropriate. It should be noted that the observed deposition patterns for sulfate for the F runs are somewhat different from those of the C runs, when the plant operating characteristics differed. In general, the F run deposition patterns, representing the scavenging under normal operating conditions, were not clearly plume-related at distances less than about 10 km.

The effect of varying K and y_{NH_3} was investigated by considering the centerline concentrations for run F3. Table 15 lists the results for various combinations of y_{NH_3} (0, 1, and 7 ppb) and K (0.0017 and 0.013 sec^{-1}). The latter value of K is that of MacKay, who arrived at that figure through a reassessment of older data[32]. The computations show that the absence of ammonia (which may also be considered an extreme case for low ammonia solubility) results in very low sulfate at all distances (the combination y_{NH_3}=0, K=0.0017, was not run, but it is clear from the other examples that this would only reduce the sulfate concentration), though the H^+ and SO_2 concentrations are more in agreement with the observations. The SO_2 concentration is, however, essentially the EPAEC-mode value, and the H^+ value is equal to that of HSO_3^-, the predominant constituent of dissolved SO_2.

The presence of ammonia, on the other hand, results in very high ammonium ion and low H^+ concentrations, with not much variation between the two values of K. From this it is highly apparent that ammonia solubility is not accounted for appropriately by this mechanism.

The quite good agreement between the EPAEC-mode (or SMICK with y_{NH_3}=0) results and the total of measured sulfur species may be evidence that some other process is occurring in the liquid phase, converting previously scavenged SO_2 to sulfate. The accuracy of the SO_2 scavenging-only model is considered to be "factor-of-two", however, so this result may be fortuitous. It should also be noted that the relationship between sulfate and H^+ concentrations does vary between runs (cf. Figure 16 comparing runs F3 and F4).

Table 15. SAMPLE SMICK PLUME CENTERLINE RAIN CONCENTRATION CALCULATIONS WITH SCOTT AND HOBBS MECHANISM: RUN F3 INPUT DATA[a]. PCO_2 = 311 ppm.

x, km	SO_2[b]	$SO_4^=$	NH_4^+	H^+
	Concentrations, (gram moles/cm^3) x 10^9			
	PNH_3 = 0	K = 0.013 sec^{-1}		
4.5	66.	0.20	0	66.
7.0	46.	0.28	0	47.
10.2	34.	0.37	0	35.
	PNH_3 = 1 ppb	K = 0.0017 sec^{-1}		
4.5	519.	2.2	531.	5.0
7.0	356.	2.9	371.	4.0
10.2	256.	3.6	274.	2.5
	PNH_3 = 1 ppb	K = 0.013 sec^{-1}		
4.5	512.	16.	551.	5.4
7.0	352.	20.	396.	3.9
10.2	251.	25.	305.	5.4
	PNH_3 = 7 ppb;	K = 0.0017 sec^{-1}		
4.5	841.	11.	944.	1.3
7.0	564.	14.	669.	0.8
10.2	403.	17.	511.	0.6

[a] See Tables 3-9.

[b] See note a, Table 14.

The cross-plume deposition pattern, as calculated by SMICK for run F3 for the Tenino area ($x \sim 10.2$ km) and for one set of y_{NH_3} and K values, is shown in Table 16. The Smith and Singer[31] sigma values appear to have been a reasonable approximation to the real plume spread in this case. The computed scavenging rates (cf. (5)) show that the same variations in magnitude occur as with the centerline concentrations.

Table 16. CROSS-PLUME SMICK RAIN CONCENTRATION CALCULATIONS: RUN F3, TENINO (x = 10.2 km) AREA. K = 0.0017 sec^{-1}; PNH_3 = 1 ppb; PCO_2 = 311 ppm.

Position	Concentration, (gram-moles/cm^3) x 10^9							
	Calculated				Observed[a]			
	SO_2[b]	$SO_4^=$	NH_4^+	H^+	SO_2[b]	$SO_4^=$	NH_4^+	H^+
Centerline	256	3.6	274	2.7	7.8[c]	23.	1.5	56.
± 5°	179	3.1	197	1.9	15.7	15.	2.5	31.
± 10°	51	1.6	70	0.7	1.8	16.	2.8	12.
± 15°	6.1	0.2	27	0.3	0.1	d	1.0	14.
± 20°	0.2	∿0	22	0.2	<0.1	d	d	5.4
± 25°	∿0	∿0	22	0.2	d	d	d	7.8
	Scavenging Rate[e], (gram moles/cm sec) x 10^9							
—	1430.	27.	1880.	20.0	85.0[c]	168.	f	988.

[a] Average of concentrations measured at approximate ± 5 degree spacings from plume centerline at Station 126 (alternate stations, except for centerline, where the average of three stations is listed).

[b] See note a, Table 14.

[c] Includes two anamolously low concentrations, see Figure 16. Thus the scavenging rate may be low.

[d] No measurement.

[e] See equation (5). Observed rates calculated from data in this table only.

[f] No deposition evident.

While the above results were derived from calculations made using T=25C, it appears that the results for lower temperatures depart further from the observations, especially in terms of NH_4^+ concentration. Limited runs using equilibrium constants corresponding to T=10C show an increase in ammonium ion concentration; this results from current knowledge of ammonia solubility, which is that the solubility increases with decreasing temperature. The resulting sulfate concentrations are probably increased as well, but these do not give much support for the efficacy of the ammonia-based model.

Thus, it appears that the Scott and Hobbs mechanism alone cannot account for the Centralia observations. Its effectiveness depends to a large degree on a significant solubility of ammonia in water, and a subsequent fast ionization. The equilibrium constants used for these processes are imperfectly known -- more research needs to be done in the area of solubility of ammonia and other gases. One cannot discount the possibility that ammonia plays a central role in more polluted environments than that of Centralia, but it appears that evidence for its action should include rather high ammonium ion concentrations and high pH in rainfall.

SECTION VIII

REFERENCES

1 Stoiber, Richard E., and Anders Jepson. Sulfur Dioxide Contributions to the Atmosphere by Volcanoes. Science 182: 577-578, 1973.

2 Kellogg, W.W., R.D. Cadle, E.R. Allen, A.A. Lazrus, and E.A. Martell. Science 175: 587, 1972.

3 Dana, M. Terry, J.M. Hales, W.G.N. Slinn, and M.A. Wolf. Natural Precipitation Washout of Sulfur Compounds from Plumes. EPA-R3-73-047. Battelle, Pacific Northwest Laboratories, Richland, WA, p. 202, June 1973.

4 Dana, M. Terry, J.M. Hales, and M.A. Wolf. Natural Precipitation Washout of Sulfur Dioxide. Battelle, Pacific Northwest Laboratories, Richland, WA, BNW-389, p. 148, February 1972.

5 Liniger, W. and R.A. Willoughby. Efficient Integration Methods for Stiff Systems of Ordinary Differential Equations. SIAM J. Numer. Anal. 7: 47-66, 1970.

6 Sherwood, C.C. and M. Berman. An Exponential Method for the Solution of Systems of Ordinary Differential Equations. Comm. of ACM 17: 699-702, 1974.

7 Carnahan, B., H.A. Luther, and J.O. Wilkes. Applied Numerical Methods. New York, Wiley, 1969.

8 Briggs, G.A. Some Recent Analyses of Plume Rise Observations. Proc. 2nd Int. Clean Air Congress, Washington, D.C., 1970.

9 Hales, J.M. Fundamentals of the Theory of Gas Scavenging by Rain. Atm. Environment 6: 635-659, 1972.

10 Scott, W.D., and P.V. Hobbs. The Formation of Sulfate in Water Droplets. J. Atmos. Sci. 24: 54-57, 1967.

11 Dana, M. Terry, J.M. Hales, and M.A. Wolf. Rain Scavenging of SO_2 and Sulfate from Power Plant Plumes. J. Geophys. Res. 80 (30): 4119-4129, 1975.

12 Dana, M. Terry and D.W. Glover. Precipitation Scavenging of Power Plant Effluents: Rainwater Concentrations of Sulfur and Nitrogen Compounds and Evaluation of Rain Sampler Desorption of SO_2. Pacific Northwest Laboratory Annual Report for 1974 to the USAEC Div. of Biomedical and Environmental Research, Part 3: Atmospheric Sciences. BNWL-1950 PT 3, Battelle, Pacific Northwest Laboratories, Richland, WA, February 1975.

13 Dana, M. Terry, J.M. Hales, C.E. Hane, and J.M. Thorp. Precipitation Scavenging of Inorganic Pollutants from Metropolitan Sources. EPA-650/3-74-005. (NTIS: PB-237 374/4G1) Battelle, Pacific Northwest Laboratories, Richland, WA, June 1974, p. 136.

14 Saltzman, B.E. Determination of Oxidants (Including Ozone): Alkaline Potassium Iodide Method. In Selected Methods for the Measurement of Air Pollutants. USHEW, Public Health Service. Cincinnati, Ohio, May 1965, pp. E-1/E-6.

15 Scaringelli, F.P., B.E. Saltzman, and S.A. Frey. Spectrophotometric Determinations of Atmospheric Sulfur Dioxide. Anal. Chem. 39: 1709, 1967.

16 Lazrus, A., E. Larange, and J.P. Lodge. New Automated Microanalysis for Total Inorganic Fixed Nitrogen and for Sulfate Ion in Water. In: Trace Inorganics in Water. ACS Advances in Chemistry Series No. 73. Washington, D.C., American Chemical Society, 1968.

17 Saltzman, B.E. Anal. Chem. 26: 1949, 1954.

18 Granat, L. On the Relation between pH and the Chemical Composition in Atmospheric Precipiation. Tellus 24: 550-560, 1972.

19 Petrenchuk, O.P., and V.M. Drozdova. On the Chemical Composition of Cloud Water. Tellus 18: 280-286, 1966.

20 Yaalon, D.H. The Concentration of Ammonia and Nitrate in Rainwater Over Israel in Relation ot Environmental Factors. Tellus 16: 200-204, 1964.

21 Tarrant, R.F., K.C. Lu, C.S. Chen, and W.B. Bollen. Nitrogen Content of Precipitation in a Coastal Forest Opening. Tellus 20: 554-556, 1968.

22 Junge, C.E. The Distribution of Ammonia and Nitrate in Rainwater over the United States. Trans. AGU 39: 241-248, 1958.

23 Jones, M.J. Ammonium and Nitrate Nitrogen in the Rainwater at Samaru, Nigeria. Tellus 23: 459-461, 1971.

24 Herman, F.A. and E. Gorham. Total Mineral Material, Acidity, Sulfur, and Nitrogen in Rain and Snow at Kentville, Nova Scotia. Tellus 9: 180-183, 1957.

25 Katz, Morris. Analysis of Inorganic Gaseous Pollutants. In Air Pollution. New York, Academic Press, 1968, pp. 55-58.

26 McCrone, W.C., R.G. Draftz, and J.G. Delly. The Particle Atlas. Ann Arbor, Ann Arbor Science Publishers, 1967.

27 Morgan, O.M. and O. Maass. Investigations of the Equilibria Existing in Gas Water Systems Forming Eloectrolytes. Can. J. Res. 5: 162-199.

28 Van den Heuval and B.J. Mason. The Formation of Ammonium Sulfate in Water Droplets Exposed to Gaseous Sulphur (sic) Dioxide and Ammonia. Quart. J. R. Meteor. Soc. 89: 271-275, 1963.

29 McConnell, J.C. Atmospheric Ammonia. J. Geophys. Res. 78 (33): 7812-7821, 1973.

30 Healy, T.V., H.A.C. McKay, A. Pilbeam, and D. Scargill. Ammonia and Ammonium Sulfate in the Troposphere over the United Kingdom. J. Geophys. Res. 75 (12): 2317-2321, 1970.

31 Smith, M.E., and I.A. Singer. An Improved Method of Estimating Concentrations and Related Phenomena from a Point Source Emission. J. Appl. Meteorol. 5: 631-639, 1966.

32 McKay, H.A. The Oxidation of Sulphur (sic) Dioxide in Water Droplets in the Presence of Ammonia. Atmos. Environ. 5: 7-14, 1971.

SECTION IX

NOMENCLATURE

Units: ℓ = length; t = time; m = mass (moles); p = pressure (atm); r = radius; none = dimensionless.

a	ℓ	Raindrop radius
a_o, a_1, a_2, a_3		Coefficients of Polynomial solved in Scott and Hobbs Mechanism
A		Subscript identifying pollutant
b		Subscript denoting "bulk"
c	m/ℓ^3	Pollutant concentration in raindrop
c_{So_2}	m/ℓ^3	SO_2 concentration in raindrop
C	m/ℓ^3	Pollutant concentration in bulk rain
H'	ℓ^3/m	Modified Henry's-law constant
i		Index integer
J	ℓ/t	Rainfall rate
K	t^{-1}	First order rate constant
K_y	$m/\ell^2 t$	Overall mass transfer coefficient based on gas driving force
n		Total number of precipitation collectors affected by plume, crosswind
P	p	Partial pressure
P_{Co_2}	p	Partial pressure of Co_2 in atmosphere
P_{NH_3}	p	Partial pressure of NH_3 in atmosphere
r_{Ax}	$m/\ell^3 t$	Reaction rate for pollutant A in rain
r_{Ay}	$m/\ell^3 t$	Reaction rate for pollutant A in air
t	t	Time
$\bar{v}_{Ax}$	ℓ/t	Velocity vector for pollutant A in rain

$\bar{v}_{Ay}$	ℓ/t	Velocity vector for pollutant A in air
v_z	ℓ/t	Terminal velocity of fall of raindrop
w_A	$m/\ell^3 t$	Counterphase transport rate of pollutant A
W	$m/\ell t$	Cross-plume integrated flux (scavenging rate)
x	ℓ	Downwind distance; also subscript denoting liquid phase
y		Crosswind distance; also subscript denoting gas phase
y_{Ab}		Mole fraction of pollutant A in gas phase
y_{NH_3}		Mole fraction of pollutant NH_3 in gas phase
y_{SO_2}		Mole fraction of SO_2 in gas phase
z	ℓ	Vertical dimension
Δz	ℓ	Vertical separation of calculation steps
ρ_{Ax}	m/ℓ^3	Molar liquid phase concentration of pollutant A in space
ρ_{Ay}	m/ℓ^3	Molar gas phase concentration of pollutant A in space
σ_y	ℓ	Plume dispersion parameter in y direction
σ_z	ℓ	Plume dispersion parameter in z direction
σ_θ	r	Plume dispersion parameter in azimuthal direction
σ_φ	r	Plume dispersion parameter in elevational direction

SECTION X

APPENDICES

		Page
A.	TABULATIONS OF RAINWATER CONCENTRATIONS, DECEMBER 1974	71
B.	THE SCOTT AND HOBBS SO_2 OXIDATION MECHANISM	79
C.	A DESCRIPTION OF THE EPAEC GAS SCAVENGING MODEL	88
D.	EXAMPLES OF Δz ADJUSTMENTS ACCOMPLISHED BY REVISED EPAEC MODEL	93

APPENDIX A

TABULATIONS OF RAINWATER CONCENTRATIONS, DECEMBER 1974

EXPLANATION OF SYMBOLS

The site numbers refer to sampling locations shown in Figure 3. The concentration data are broken into groups corresponding to the general sampling areas identified in Table 1. Where the rainfall amount column is blank, no sample was taken. Blanks in other columns indicate that no analysis was performed. The symbol "<" means that the measured concentration was less than the lower detection limit for that particular specie during the analysis session. "$\leq$" means that the following number is an upper limit on the concentration, as a result of analysis difficulties or other uncertainty. "NE" means that there was not enough water sample remaining to conduct the analysis.

TABLE 17: RAIN SAMPLE CONCENTRATION DATA: RUN F1, DECEMBER 6, 1974

Site #	Rainfall cm	Concentration (gram-moles/cm^3) x 10^9						
		SO_2	$SO_4^=$	NO_2^-	NO_3^-	NH_4^+	H^+	PO_4^{3-}
BKG	.04	0.2					NE	NE
1	.12	≤.2			5.6	1.9	66.	0.054
2	.11	0.1					44.	
3	.13	0.2			4.6	2.7	42.	
4	.11	≤.2					4.5	
5	.12	0.1			3.8	4.4	91.	0.027
6	.10	0.1					60.	
7	.11	0.2			5.0	3.6	3.6	0.134
8	.10	0.4					39.	
9	.08	0.3			5.1	4.0	91.	NE
10	.08	1.2			2.9	4.5	32.	NE
11	.09	1.2			4.3	3.3	91.	
12	.09	0.8			4.8	3.2	8.5	
13	.08	0.2					41.	
14	.08	0.2					7.4	
15	.08	0.1					54.	
16	.08	0.2			2.6	4.4	7.4	NE
17	.08	≤.1					9.3	
18	.08	≤.1					3.6	
19	.06	0.4					1.9	
59								
60								
61	.80	≤.1		0.04			55.	
62	.77	≤.1		0.06			66.	
63	.83	≤.1		0.08			58.	
64	.70	≤.1		0.08	2.1	2.0	63.	0.074
65	.45	≤.1		≤.03			55.	
66	.41	≤.1		0.15			78.	
67	.22	≤.1		0.31	3.5	2.9	40.	0.142

Table 17 (Continued)

68	.22	0.1		0.19			53.		
69	.16	<.1		0.05			3.2		
70	.25	0.2		0.30	9.0	3.3	14.	0.047	
71	.27	<.1	24.	0.07			60.		
72	.35	<.1		0.03	3.6	3.5	53.	0.033	
73	.39	0.5	29.	0.04	2.7	2.2	74.	0.049	
74	.61	0.9		0.04			69.		
75	.93	2.1		0.04		2.0	53.	0.026	
76	.96	3.3		0.03	2.2	2.3	81.	<.01	
77									
78	.56	0.5		0.04	2.8	2.4	40.	0.030	
79	.51	<.1		0.05	2.8	2.0	51.	0.020	
80	.17	0.2	28.	0.13	2.7	7.1	62.	0.080	
81	.26	0.2	33.	0.21	3.8	2.5	40.	0.078	
82	.30	<.2	16.	0.03	2.5	3.7	87.	0.117	
83	.33	<.2		<.03			87.		
84	.31	1.1		0.07	4.6	4.0	76.	0.070	
85	.23	1.1		0.14			79.		
86	.22	1.0		0.06			81.		
87	.17	0.9		0.06			100.		
88									
89	.16	2.7	20.	0.03	4.0	4.0	83.	0.022	
90	.33	1.8		<.03			85.		
91	.35	1.4		0.07	4.8	4.3	45.		
92	.24	1.4		<.03			60.		
93	.25	1.0		<.03	2.6	1.7	87.	0.044	
94	.49	0.2		0.04			83.		
95	.36	<.2		<.03			100.		
96	.27	0.2		0.13			74.		
97									
98	.09	0.5			6.8	6.8	79.	0.155	
99									
100									

Table 17 (Continued)

101								
102								
120	.54	<.1	16.	0.07	1.8	2.6	10.	<.02
121	.53	<.1		0.08			48.	
122	.48	<.1		0.07			83.	
123	.38	<.1		0.10			71.	
124	.39	<.1	15.	0.06	1.8	2.4	56.	0.024
125	.28[a]	<.1		0.07	1.2	3.4	4.9	0.019
126	.32	<.1		0.09			56.	
127	.33	<.1		0.07	2.3	3.9	7.6	0.020
128	.10[a]	0.3		0.12			91.	
129	.32	0.2		0.07			91.	
130	.12[a]	1.3	34.	0.09	3.6	0.9	11.	
131	.31	0.6		0.08			63.	
132	.33	0.5		0.04	3.0	3.4	76.	0.018
133	.35	0.8		<.03			112.	
134	.34	0.6		0.04			87.	
135	.13[a]	1.5	43.	0.05	3.4	3.5	102.	0.041
136	.38	1.0		0.12			16.	
137	.42	0.3		0.09	3.4	2.3	96.	0.020
138	.45	1.0		0.05			12.	
139	.38	1.0		<.03	2.7	2.2	85.	0.022
140	.31	0.7		0.10			76.	
141	.29	0.7		0.17	1.9	4.7	8.3	0.022
142	.07[a]	2.0					96.	
143	.45	<.1		0.04	2.7	1.4	33.	<.01
144	.62	<.1		0.13	2.4	4.7	69.	<.01
145	.03[a]	0.9					NE	

[a] Incomplete sample due to water freezing in neck of funnel. Thus, the rain analyzed came early in the run.

TABLE 18: RAIN SAMPLE CONCENTRATION DATA: RUN F3, DECEMBER 10, 1974

Site #	Rainfall cm	Concentration (gram-moles/ℓ) x 10^6						
		SO_2	$SO_4^=$	NO_2^-	NO_3^-	NH_4^+	H^+	PO_4^{3-}
BKG	0.06	<.1			4.5	1.7	7.4	
1	0.14	0.21					4.9	
2	0.11	0.25			3.1	<.5	4.5	0.033
3	0.16	0.17		0.13			5.1	
4	0.17	0.21		0.10	3.0	<.5	53.	0.029
5	0.13	0.23			2.3	≤.5	5.1	
6	0.15	1.6		0.04	2.8	≤.5	65.	
7	0.16	5.7	18.	0.10	1.6	1.7	25.	
8	0.16	9.8	10.		1.8	3.4	34.	
9	0.14	10.6	12.	0.09	2.9	3.0	69.	
10	0.14	3.4	7.1		1.9	1.1	36.	0.059
11	0.13	0.25					12.	
12	0.15	0.10	<2.		2.1	<.5	9.1	
13	0.13	<.1					12.	
14								
15								
16								
17								
18								
19								
59								
60	0.29	32.7	6.6	<.03	2.1	≤1.0	69.	
61	0.27	<.1	<2.	0.04	0.8	1.2	5.9	≤.01
62	0.26	<.1	4.4	0.03			7.6	
63	0.30	<.1		<.03			45.	
64	0.34	<.1		0.03	2.4	1.6	6.2	
65	0.33	<.1		0.03			20.	
66	0.33	<.1		<.03	1.0	2.0	6.0	<.015
67	0.29	<.1		<.03			44.	

Table 18 (Continued)

68	0.34	<.1		0.03			58.	
69	0.36	<.1	14.	<.03	1.5	≤.9	8.5	
70	0.32	15.1	8.3	<.03	1.7	≤.6	74.	0.016
71	0.29	33.0	14.	<.03	0.9	2.4	76.	0.044
72	0.28	11.8	3.4	<.03	2.2	1.2	28.	0.088
73	0.23	<.1	13.	0.04	2.1	<.5	23.	<.015
74	0.23	<.1		0.05			50.	
75	0.23	0.48		0.23			36.	
76	0.21	<.1		0.05			11.	
77	0.20	<.1		0.10			4.2	
78	0.18	<.1		0.15			3.5	
79	0.18	<.1		0.10			58.	
80	0.26	24.9	6.8	0.08	2.1	6.7	26.	
81	0.35	17.4	<2.	0.05	0.3	6.9	20.	0.063
82	0.32	9.7	28.	<.03	0.8	2.3	74.	0.038
83	0.27	27.7	13.	0.06	2.8	3.6	34.	
84	0.34	3.3	11.	0.03	1.9	1.8	47.	
85	0.31	<.1		0.08			40.	
86	0.33	<.1		0.07			8.3	
87	0.13	<.1		0.15	1.9	9.0	5.4	
88								
89	0.29	<.1		0.13			10.	
90	0.22	0.10		0.17	1.5	4.0	26.	
91	0.28	<.1		0.12	2.2	4.5	24.	
92	0.32	<.1		0.07	1.9	3.5	16.	
93	0.31	0.10		0.10	2.2	1.7	20.	
94	0.22	0.15		0.23	1.9	4.9	15.	
95								
96								
97								
98	0.19	2.1	7.8	0.08	0.4	5.5	18.	
99	0.32	13.2	9.3	0.04	1.2	7.4	68.	0.030
100	0.28	0.21	9.0	0.09	1.9	2.1	8.5	0.018

Table 18 (Continued)

101								
102								
120	0.41	<.1		0.09	1.2	1.8	4.8	
121	0.35	0.11		0.09	1.6	1.0	22.	0.050
122	0.18	3.6	8.0	0.15	1.3	4.7	14.	
123	0.34	12.4	8.0	0.03	0.9	1.1	20.	<.012
124	0.44	17.9	6.8	0.06			42.	
125	0.37	0.17	33.	0.05	1.8	0.9	60.	
126	0.42	1.6	31.	0.06	0.8	2.3	63.	<.01
127	0.36	21.5	4.9	0.04	0.5	1.4	45.	0.026
128	0.37	13.5	22.	0.04	0.8	2.5	20.	
129	0.34	5.3	13.	0.03	0.5	2.2	16.	0.024
130	0.37	<.1	23.	0.03	1.3	1.0	10.	0.020
131	0.37	<.1		0.06			6.9	
132	0.36	<.1		0.12			6.5	
133	0.38	<.1		0.06			5.1	
134	0.07	<.1		0.11			6.0	
135	0.40	<.1		0.10			5.1	
136	0.37	0.10		0.04			7.8	
137								
138	0.31	<.1		0.09			5.9	
139	0.20	0.15		0.11	1.9	1.5	19.	
140	0.30	<.1		0.09			6.8	
141	0.23	0.10		0.17			4.9	
142								
143								
144								
145								

TABLE 19: RAIN SAMPLE CONCENTRATION DATA: RUN F4, DECEMBER 12, 1974

Site #	Rainfall cm	Concentration (gram-moles/cm^3) x 10^9						
		SO_2	$SO_4^=$	NO_2^-	NO_3^-	NH_4^+	H^+	PO_4^{3-}
BKG	0.38	<.10	14.	0.05	0.9	1.8	4.3	
1	0.40	0.16	<4.	0.11			5.5	
2	0.42	<.10	<4.	0.08			4.8	
3	0.42	<.10	<3.	0.10	0.7	1.2	4.0	
4	0.40	<.10		0.04	2.0	<.5	36.	<.01
5	0.40	<.10	9.4	0.11	1.0	1.0	5.0	<.01
6	0.41	<.10		0.03	1.0	0.9	6.8	
7	0.40	<.10		0.03	0.4	1.4	8.9	
8	0.40	2.1	9.0	0.04	0.8	1.2	25.	
9	0.41	9.4	21.	<.03	1.1	<.5	78.	0.024
10	0.39	14.9	17.	0.08	0.5	1.0	55.	
11	0.38	18.7	8.9	0.03	<.5	1.9	81.	0.046
12	0.44	1.5	12.	0.04	0.9	1.0	49.	
13	0.42	6.9	18.	0.03	2.0	<.5	17.	
14	0.45	4.6	14.	0.06	0.7	<.6	15.	
15	0.41	1.8	7.3	<.03	1.1	0.7	11.	
16	0.43	<.10	<4.	0.04			6.5	
17	0.39	<.10	<4.	0.14			6.6	
18	0.37	<.10	11.	0.06			8.3	
19	0.39	<.10	18.	0.08			3.2	
59								
60	0.17	0.77	8.2	0.28	0.7	18.1	44.	
61	0.49	<.10	<3.	0.11	<.4	3.7	6.9	
62	0.51	<.10		0.04			10.	
63	0.48	<.10	14.	0.06			7.1	
64	0.47	<.10	7.3	0.16	<.3	6.5	8.1	
65	0.41	<.10		0.11			6.6	
66	0.35	<.10	6.0	0.11	2.8	4.0	8.9	0.047
67	0.25	0.20	<3.	0.13			23.	

Table 19 (Continued)

68	0.22	0.10	10.	0.14			21.	
69	0.17	<.10	20.	NE			10.	
70	0.18	0.22	15.	0.21	1.5	8.1	8.3	
71	0.14	7.8	20.	NE	3.6	19.0	15.	
72	0.10	9.0	24.	NE	4.0	19.5	27.	0.050
73	0.08	0.22		NE	4.2	18.6	5.9	
74	0.06	0.18	22.	NE			44.	
75	0.07	0.15	14.	NE	6.9	9.6	16.	
76	0.08	0.40	23.	NE			1.9	
77	0.07	0.36	15.	NE			3.5	
78	0.09	0.10		NE			9.3	
79	0.09	0.25	26.	NE			8.1	
80	0.42	18.2	7.0	<.03	0.6	2.2	30.	
81	0.38	17.1	17.	0.04	<.5	5.0	26.	<.01
82								
83								
84								
85								
86								
87								
88								
89								
90								
91								
92								
93								
94								
95								
96								
97								
98	0.37	16.1	16.	<.03	<.5	4.5	26.	0.011
99								
100								

Table 19 (Continued)

101								
102	0.34	12.3	5.9	<.03	1.7	3.7	21.	
120	0.22	<.10	≤4.	0.07	1.1	4.4	23.	
121	0.24	<.10	11.	0.21			5.1	
122	0.23	<.10		0.07	1.3	4.9	17.	0.039
123	0.25	0.73	12.2	0.06	1.2	2.8	10.	
124	0.26	5.8	21.	<.03	1.7	2.0	16.	<.01
125	0.22	10.5	22.	0.06	0.7	2.9	20.	
126	0.23	10.8	22.	0.04	0.7	6.5	24.	
127	0.21	10.9	22.	0.08	1.3	3.7	26.	0.022
128	0.18	10.1	13.	0.08	2.3	3.9	17.	
129	0.17	8.7	22.	0.06	1.5	4 0	17.	
130	0.17	4.5	11.	0.04	0.6	3.5	12.	
131	0.16	2.9		0.06			12.	
132	0.16	2.3	9.5	0.12	1.7	7.0	7.6	
133	0.16	1.8	9.4	0.19	2.1	7.4	7.9	0.030
134	0.13	1.5	19.	0.29			2.4	
135	0.12	0.76	16.		2.4	4.7	7.2	0.016
136	0.11	0.40	16.	0.18			6.3	
137	0.10	0.47	15.	NE			24.	
138	0.09	0.71	23.	NE			1.6	
139	0.10	0.25	22.	NE			32.	
140	0.06	0.31	19.	NE			3.3	
141	0.05	0.73		NE			8.5	
142								
143								
144								
145								

Table 20. RAIN SAMPLE CONCENTRATION DATA: RUN F5; DECEMBER 15, 1974

Station	Rainfall	Concentration (gram-moles/cm^3 X 10^9)						
	cm	SO_2	$SO_4^=$	NO_2^-	NO_3^-	NH_4^+	H^+	PO_4^{3-}
Bkg	0.02	<0.05	<3.				8.9	
80	0.02	0.69	30.				24.	
81	0.03	1.3	33.				21.	
82	0.02	4.7	45.				71.	
84	0.01	0.47	27.				11.	
98	0.02	0.61	22.				45.	
102	0.02	0.45	32.				42.	
126	0.02	4.6	41.				33.	
127	0.02	6.3	57.				29.	
128	0.02	3.1	77.				110.	
129	0.02	1.5	55.				79.	
130	0.03	0.22	40.				96.	
133	0.02	1.2	33.				4.6	
136	0.04	0.34	48.				50.	

Table 21. CONCENTRATION RESULTS - MOBILE SAMPLES (AND ASSOCIATED FIXED SITES): RUN F3, DECEMBER 10. 1974

Site	Desig.	Time[a] PST	Duration min	Rainfall Rate mm/hr	Concentration (gram-moles/cm^3) x 10^9 SO_2	$SO_4^=$	NO_2^-	NO_3^-	NH_4^+	H^+ (pH)
71	A	1350	10	0.38	38.	88	0.09	5.5	3.3±.6	48.(4.32)
	B	1400	15	0.74	22.	41	<.03	5±.8	≤1.7	20.(4.70)
	C	1415	15	0.62	11.	40	0.10	≤2.0	≤0.5	31.(4.51)
	D	1430	10	1.6	3.3	21	<.03	1.9	≤0.8	11.(4.97)
	E	1445	3	0.74	8.2	99		≤0.6	≤0.8	85.(4.07)
59[b]	A	1515	15	1.1	13.	24	<.03	1.3	≤0.8	26.(4.59)
71	(Fixed)	1302	182	1.0	33.	14	<.03	0.9	2.4	76.(4.12)
82	A	1501	6	1.0	28.	56	<.03	0.6	1.4	68.(4.17)
	B	1510	7.5	0.31	52.	59		≤1.3	≤0.8	87.(4.06)
	C	1520	7	1.0	57.	56	<.03	≤1.2	≤0.8	96.(4.02)
	D	1533	5	0.68	60.	73	<.03	<0.6	≤0.8	129.(3.89)
82	(Fixed)	1252	170	1.1	9.7	28	<.03	0.8	2.3	74.(4.13)
101	A	1437	1.5	3.4	<0.1	22	0.05	1.9	<0.8	31.(4.51)
	B	1442	1.	6.3	<0.25	26	0.04	<0.6	<0.8	46.(4.34)
	C	1449	3	0.44	<0.25	21		1.4	<0.8	7.2(5.14)
84	(Fixed)[c]	1258	178	1.1	3.3	11	0.03	1.9	1.8	47.(4.33)
100	(Fixed)[d]	1324	174	1.0	0.21	9	0.09	1.9	2.1	8.5(5.07)

[a] At start of sample

[b] 0.7 km W of Site 71

[c] 0.2 km S of Site 101

[d] 0.2 km N of Site 101

Table 22. CONCENTRATION RESULTS - MOBILE SAMPLES (AND ASSOCIATED FIXED SITES): RUN F4, DECEMBER 12, 1974

Site	Desig.	Time[a] PST	Duration min	Rainfall Rate mm/hr	Concentration (gram-moles/cm^3) x 10^9 SO_2	$SO_4^=$	NO_2^-	NO_3^-	NH_4^+	H^+ (pH)
66	A	1017	3	2.6	1.0	19	0.14	0.5	4.6	6.5(5.19)
66	Fixed	1030	247	2.7[b]	<0.1	6.0	0.11	2.8	4.0	8.9(5.05)
71[c]	F	1032	2	6.9	13.	25	<.03	1.0±.6	≤1.2	21. (4.68)
	G	1245	10	0.76	21.	72	0.06	5.7	5.3	96. (4.02)
	H	1300	15	0.16	11.	58	-	5.5	2.6±1	59. (4.23)
	I	1315	8	0.24	3.8	45	-	5.8	4.3±1	33. (4.48)
71	Fixed	1054	198	1.5[b]	7.8	20	-	3.6	19.	15. (4.82)
73	A	1046	2.5	3.5	4.1	8	-	0.9	≤0.8	22. (4.65)
73	Fixed	1103	183	1.1[b]	0.22	-	-	4.2	19.	5.9(5.23)
82	E	1221	∿3	∿0.6	22.	47	-	2.5	4.9	78. (4.11)
	F	1258	3.5	1.3	14.	57	<.03	4.6	3.6	71. (4.15)

a Time of beginning sample

b Based on time of rainfall of Site 9

c Actually 0.15 km E of Site 71

Table 23. CONCENTRATION RESULTS - MOBILE SAMPLES: CONVECTIVE SHOWER, DECEMBER 12, 1974

Site	Desig.	Time[a]	Duration	Rainfall Rate	Concentration (gram-moles/cm^3) x 10^9					
		PST	min	mm/hr	SO_2	$SO_4^=$	NO_2^-	NO_3^-	NH_4^+	H^+ (pH)
10	A	1429	3	2.1	<0.1	23	<.03	3.6	6.3	14.(4.85)
12	A	1438	0.5	30.	3.6	19	<.03	2.3	4.8	31.(4.51)
14	A	1443	2	6.4	22.	34	<.03	3.3	10.	76.(4.12)
16	A	1449	3	2.5	14.	40	<.03	3.8	11.	48.(4.32)
18	A	1458	3	1.5	65.	25	<.03	0.2	2.8	126.(3.90)
20	A	1506	b	b	64.	24	<.03	<.6	1.2	78.(4.11)
16	B	1517	4	0.30	18.	46	-	2.5	<.8	96.(4.02)

[a] Time at beginning of Sample

[b] Unknown

APPENDIX B

THE SCOTT AND HOBBS MECHANISM

This mechanism[10] is based on the assumption that the oxidation of SO_2 is catalyzed by ammonia. The following equilibria are involved:

$$SO_2(gas) + H_2O \rightleftharpoons SO_2 \cdot H_2O \quad (6a)$$

$$SO_2 \cdot H_2O \rightleftharpoons H^+ + HSO_3^- \quad (7a)$$

$$HSO_3^- \rightleftharpoons H^+ + SO_3^= \quad (8a)$$

$$NH_3(gas) \rightleftharpoons NH_3 \cdot H_2O \quad (9a)$$

$$NH_3 \cdot H_2O \rightleftharpoons NH_4 + OH^- \quad (10a)$$

$$CO_2(gas) \rightleftharpoons CO_2 \cdot H_2O \quad (11a)$$

$$CO_2 \cdot H_2O \rightleftharpoons H^+ + HCO_3^- \quad (12a)$$

$$HCO_3^- \rightleftharpoons H^+ + CO_3^= \quad (13a)$$

$$H_2O \rightleftharpoons H^+ + OH^-. \quad (14a)$$

The corresponding equilibrium constants are defined:

$$K_{hs} = [SO_2 \cdot H_2O]/P_{SO_2} \quad (6b)$$

$$K_{1s} = [H^+][HSO_3^-]/[SO_2 \cdot H_2O] \quad (7b)$$

$$K_{2s} = [H^+][SO_3^=]/[HSO_3^-] \quad (8b)$$

$$K_{ha} = [NH_3 \cdot H_2O]/P_{NH_3} \quad (9b)$$

$$K_{1a} = [NH_4^+][OH^-]/[NH_4^+ \cdot H_2O] \quad (10b)$$

$$K_{hc} = [CO_2 \cdot H_2O]/P_{CO_2} \quad (11b)$$

$$K_{1c} = [H^+][HCO_3^-]/[CO_2 \cdot H_2O] \quad (12b)$$

$$K_{2c} = [H^+][CO_3^{--}]/[CO_2 \cdot H_2O] \quad (13b)$$

$$K_w = [H^+][OH^-]. \quad (14b)$$

The numerical values used in the calculations (Section VII) are listed in Table 24.

In the above expressions the brackets indicate molar concentrations, and P is partial pressure in the atmosphere.

The SO_2 oxidation is assumed to be first order:

$$\frac{d[SO_4^{=}]}{dt} = K[SO_3^{=}]. \tag{15}$$

For the sake of electroneutrality,

$$[H^+] + [NH_4^+] =$$

$$[HSO_3^-] + 2[SO_3^{=}] + 2[SO_4^{=}] + [HCO_3^-] + 2[CO_3^{=}] + [OH^-] \tag{16}$$

By rearranging expressions (6)-(14) and defining

$$c_{SO_2} = [HSO_3^-] + [SO_2 \cdot H_2O],$$

(16) yields and equation for $[H^+]$:

$$a_3[H^+]^3 + a_2[H^+]^2 + a_1[H^+] + a_o = 0, \tag{17}$$

where

$$a_3 = -1 - K_{ha}K_{1a}P_{NH_3}/K_w \tag{18}$$

$$a_2 = 2[SO_4^{=}] - K_{1s} - K_{ha}K_{1a}P_{NH_3}K_{1s}/K_w \tag{19}$$

$$a_1 = K_{1s}c_{SO_2} + 2[SO_4^{=}]\,K_{1s} + K_{hc}K_{1c}P_{CO_2} + K_w \tag{20}$$

$$a_o = K_{ks}(2K_{2s}c_{SO_2} + K_{hc}K_{1c}P_{CO_2} + K_w) \tag{21}$$

It has been assumed that $[CO_3^{=}]$ is negligible. The subroutine to SMICK which solves (17) for $[H^+]$ uses a cubic equation-solving subroutine and then calculates $[HSO_3^-]$, $[SO_3^{=}]$, $[NH_3 \cdot H_2O]$, $[NH_4^+]$, $[CO_2 \cdot H_2O]$, $[HCO_3^-]$, $[CO_3^{=}]$, and

$$[H^+]_{ex} = [H^+] - [HSO_3^-] =$$

$$2([SO_3^{=}] + [SO_4^{=}] + [CO_3^{=}] + [HCO_3^-] + [OH^-] - [NH_4^+]. \tag{22}$$

The value for $[SO_4^{=}]$ is found by integrating (15), and the value of c_{SO_2} is found by integrating the differential equation for absorption by the falling drop ((1)).

The use of this mechanism in SMICK does not follow Scott and Hobbs[10] procedure of assuming an SO_2(gas) - SO_2 (aqueous) equilibrium. Furthermore, the introduction of ammonia into the system leads to the possibility that $[HSO_3^-] > [H^+]$; thus $[H^+]_{ex}$ can be negative. This occurrence makes it necessary to continually recalculate the value of this variable for use where needed elsewhere in SMICK.

Table 24. VALUES OF THE EQUILIBRIUM CONSTANTS (Equations 6b-14b) USED IN SMICK CALCULATIONS WITH THE SCOTT AND HOBBS MECHANISM (T=298K).

Constant	Value Used	
K_{hs}	0.00124	moles/cm^3
K_{1s}	1.27×10^{-5}	moles/cm^3
K_{2s}	6.24×10^{-11}	moles/cm^3
K_{ha}	0.057	moles/cm^3
K_{1a}	1.77×10^{-8}	moles/cm^3
K_{hc}	3.4×10^{-5}	moles/cm^3
K_{1c}	4.45×10^{-10}	moles/cm^3
K_{2c}	4.68×10^{-14}	moles/cm^3
K_w	1.01×10^{-20}	(moles/cm^3)^2

APPENDIX C

A DESCRIPTION OF THE EPAEC GAS SCAVENGING MODEL

A detailed description of the model, with computer listing and glossary of terminology, appears in another report[3]. This appendix is to provide a brief review of the gas scavenging theory involved, and a summary of the calculation scheme of EPAEC, as background for the discussion of the modifications to EPAEC in Section IV.

The basis for all washout calculations for present purposes is the property that a gas will be absorbed or desorbed depending upon whether the concentration driving force is to or away from the falling raindrop. Mathematically, this may be expressed by the form

$$N_{Ao} = -K_y(y_{Ab} - y_{Ae}) \quad , \tag{23}$$

where N_{Ao} is the flux of pollutant A away from the drop at its interface. The subscripts A and o denote "pollutant A" and "interface," respectively, in a manner consistent with terminology used in a more detailed account[9]; the subscript b denotes "bulk," indicating that the entity being described is an average or "mixed-mean" value, and y_{Ab} is the mole fraction of A in the local gas phase. y_{Ae} is the mole fraction of A in the liquid phase expressed in gas-phase terms to allow incorporation with y_{Ab} as a driving force; it is, more precisely, the gas-phase mole fraction that would coexist in equilibrium with the mixed-mean mole fraction in the liquid phase x_{Ab}.

The above equilibrium relationship can be expressed by the functional form

$$y_{Ae} = h(x_{Ab}) \quad . \tag{24}$$

In the event that the gas-phase fraction is linearly dependent on the liquid-phase value, the above equation reduces to

$$y_{Ae} = Hx_{Ab} \quad , \tag{25}$$

where H is the Henry's-law constant. This may be expressed in terms of liquid-phase concentration by the essentially equivalent form

$$y_{Ae} = H'c_{Ab} \quad , \tag{26}$$

where $H' = H/c_x$ is a modified Henry's-law constant, c_x being the total liquid-phase concentration (nominally 1/18 moles/cm^3). Nonlinear behavior in the equilibrium relationship is accounted for in the numerical model simply by applying the form (26) and varying H' as the computation progresses.

To calculate washout concentrations one must rewrite (23) in terms of the liquid-phase concentration, c_{Ab} (abbreviated to c in Section IV). The result is

$$\frac{dc_{Ab}}{dz} = \frac{3K_y}{v_z a}(y_{Ab} - H'c_{Ab}) \quad , \tag{27}$$

where K_y is the overall mass-transfer coefficient, and v_z is the terminal fall velocity of a raindrop of radius a.

Mass-transfer coefficients for gas absorption by falling drops have been the subject of extensive discussion in the literature. The EPAEC model considers limiting conditions, namely those posed by gas-phase limited and stagnant drop behavior. Behavior of real systems should fall somewhere between these extreme cases.

The gas-phase mass-transfer coefficient k_y can be estimated from the well-known Froessling equation

$$\frac{2k_y a}{D_{Ay}c_y} = 2 + 0.6\left[\frac{-2av_z}{\nu}\right]^{0.5}\left[\frac{\nu}{D_{Ay}}\right]^{0.33} \quad , \tag{28}$$

where D_{Ay} is the diffusivity of SO_2 in air, c_y is the total concentration in the gas-phase, and ν is kinematic viscosity of air. For stagnant drop conditions the liquid-phase mass transfer coefficient can be calculated using published solutions to the continuity equation describing diffusion into a sphere. Although the resulting values are concentration dependent, they can be approximated by constant values corresponding to drops experiencing ramp-function

changes in surface concentrations,[9] thus,

$$k_x = \frac{5D_{Ax}c_x}{a} \tag{29}$$

where D_{Ax} is the molecular diffusivity of SO_2 in water.

Equations (28) and (29) may be used to calculate the overall coefficient for the limiting cases using the well-known relationship

$$K_y = \frac{1}{\frac{H'c_x}{k_x} + \frac{1}{k_y}} \quad . \tag{30}$$

An appropriate form for the gas-phase concentration field $y_{Ab}(x,y,z)$ must be furnished prior to calculation of numerical results. At the present time this procedure uses Pasquill-Gifford bivariate-normal plume equation, modified to account for pseudo first-order chemical reaction (of rate k) and background. This is given as

$$y_{Ab} = \frac{Q}{2\pi\sigma_y\sigma_z\bar{u}} \exp[-1/2(\frac{y}{\sigma_y})^2]\{\exp[-1/2(\frac{z-h}{\sigma_z})^2] + \exp[-1/2(\frac{z+h}{\sigma_z})^2]\}$$

$$\exp(-\frac{kx}{\bar{u}}) + y_{Ab}|_{bkg} \quad . \tag{31}$$

The solubility of a gas in water often depends upon concentration in a highly non-linear fashion. This is true for SO_2: our previous laboratory measurements have shown the relationship to be given approximately by the form

$$c_{SO_2} = [SO_2]_{aq} + [HSO_3^-]$$

$$= \frac{[SO_2]_g}{H^o} + \frac{-[H_3O^+]_{ex} + \sqrt{[H_3O^+]_{ex}^2 + 4K_1[SO_2]_g/H^o}}{2} \quad , \tag{32}$$

where the bracketted terms denote concentrations in moles/liter and $[H_3O^+]_{ex}$ is the concentration in solution of hydrogen ions donated by sources other than the SO_2 ionization reaction. H^o and K_1 are the ("true") Henry's-law and dissociation constants, respectively, for reactions (33) and (34):

$$H^{\circ} = \frac{[SO_2]_g}{[SO_2]_{aq}} \quad , \tag{33}$$

$$K_1 = \frac{[HSO_3^-][H_3O^+]_{total}}{[SO_2]_{aq}} \quad . \tag{34}$$

Here it is important to note that $[SO_2]_{aq}$ denotes dissolved, undissociated SO_2, while the total dissolved SO_2 is denoted by c_{SO_2}.

Execution of the EPAEC model consists simply of solving (27) numerically, in conjunction with subroutine - provided values of K_y, v_z, y_{Ab}, and H'*, for a number of selected drop sizes, and then distributing the results according to the raindrop spectrum to obtain average concentrations. The computer code performs this function and allows for a number of sophistications including nonlinear solubility behavior, lofting plumes, and nonvertical rainfall.

Prior to entering the integration algorithm, an "equilibrium scavenging" test is performed. This test determines whether or not the expected liquid-phase concentration (within a drop of particular radius a) at the receptor location is that which would be in equilibrium with the local gas-phase concentration. In the former case, the liquid-phase concentration c_{Ab} is set to

$$c_{Ab} = y'_{Ab}/H'(y'_{Ab}) \quad , \tag{35}$$

where y'_{Ab} is the air concentration at the receptor location, and the integration is bypassed. Otherwise, (27) is integrated along a slanted raindrop trajectory (determined by the wind speed and the terminal fall velocity), beginning at a selected point above the plume** and ending at ground level or other selected receptor elevation. The integration is performed with a fourth-order Runge-Kutta algorithm, which provides values of c_{Ab} in response to pro-

*The identity of the gas essentially only appears in H'. Thus an H' subroutine for any gas may be used.

**Where y_{Ab} is 0.01 of the centerline value with the plume rise and raindrop trajectory accounted for.

vided values of dc_{Ab}/dz. The exprected errors from this method are of the order of the fractional grid spacing to the fourth power.

The receptor-level value of c_{Ab} is returned to the main program, and the process is repeated for the rest of the preselected raindrop sizes. The average concentration is determined by summing over the raindrop spectrum *via*

$$c_{avg} = \frac{\sum_{1}^{N} F_i D_i^3 c_{Abi}}{\sum_{1}^{N} F_i D_i^3} \quad , \tag{36}$$

where D_i and F_i are the diameter and frequency of the ith drop size, and N is the total number of different drop sizes.

The input chemical and meteorological conditions are printed out, along with concentrations for each drop size and the average. If desired, the program can calculate at a number of cross-plume (y-dimension) positions and perform calculations of cross-plume integrated flux ("scavenging rate", cf. (5)) at any desired number of downwind distances.

APPENDIX D

EXAMPLES OF ΔZ ADJUSTMENTS ACCOMPLISHED BY REVISED EPAEC MODEL

As in the original version of EPAEC, the starting point for integration (X_T, Y_T, z_T) is calculated prior to beginning the integration. This starting point is that where the drop first encounters an air concentration of the pollutant which is some fraction of that at the plume centerline (e.g., $y_{Ab}(X_T, Y_T, z_T) \simeq 0.01\ y_{Ab}(X_T, Y_T, H)$, or $z_T \simeq H + 3\sigma_\varphi X_T$); (X_T, Y_T, z_T) is a function of windspeed u, raindrop terminal velocity v_z (and thus radius a), source height H, sampling distance x_B, $\sigma_\varphi(z)$, and plume loft. The stack intercept, or distance above the source point that the drop crosses the (x, y) plane, is given by

$$S = \frac{-X_B V_z}{u} - H \quad . \tag{37}$$

If S < 0 ("undercutting"), z_T is set equal to S+H, and Δz, the computational grid spacing in the z direction, is $z_T/40$. If S > 0 and there is no plume loft,

$$X_T = \frac{S}{\frac{V_z}{u} - 3\sigma_\varphi} \quad , \tag{38}$$

$$Z_T = H + S + X_T V_z/u \quad , \tag{39}$$

and

$$\Delta z = \frac{X_T \sigma_\varphi}{5} \quad . \tag{40}$$

Thus, the number of integration levels N, is

$$N \simeq -z_T/\Delta z \quad . \tag{41}$$

Table 25 lists input data for two sets of computations where I_2 was the pollutant gas (the solubility properties are similar to those of SO_2); the only difference between them is the source strength Q. Table 26 shows some of the results. The values of N actually used (in the non-equilibrium scavenging

cases) vary both above and below the initially set values. More integration steps are required for the higher value of Q because the solubility of I_2 (as with SO_2) is lower (higher value of H'); but the equilibrium scavenging criterion is met for larger drop sizes, for this particular set of input conditions at least. In the case of the more-stably-integrating lower Q runs, the spacing could be reduced for all appropriate drop sizes.

Table 25. INPUT DATA FOR SAMPLE CALCULATIONS

Source Strength	Q	1×10^{-5} and 0.1	moles/sec
Source Height	H	6000	cm
Sampling Distance	X_B	2×10^4	cm
Wind Speed	u	500	cm/sec
	σ_φ	0.157	radians

Table 26. SAMPLE CALCULATIONS SHOWING Δz VARIATION

DROP DIAMETER cm	V_z cm/sec	Initially Calculated S cm	X_T cm	z_T cm	Δz cm	N	Actually used in Computation N(Q = 0.1)	N(Q = 10^{-5})
0.019	-67.7	-3290	0	2710	68	40	0[a]	0[a]
0.026	-99.1	-2040	0	3970	99	40	0[a]	0[a]
0.035	-139.	- 429	0	5570	139	40	0[a]	0[a]
0.047	-192.	1680	1960	6930	62	112	0[a]	0[a]
0.064	-264.	4560	4570	8150	144	57	0[a]	0[a]
0.087	-355.	8190	6940	9270	218	43	0[a]	26
0.118	-459.	12400	8900	10200	280	36	0[a]	22
0.160	-566.	16600	10400	10900	326	33	62	20
0.215	-682.	21300	11600	11500	365	31	42	19
0.295	-800.	26000	12500	11900	395	30	19	19

[a] The integration was bypassed into the "equilibrium scavenging" calculation.